Effect of mini-implant collar design on orthodontic skeletal anchorage

Master of Science Candidate: Holly J. Grimslid, DMD

A thesis submitted to the Department of Orthodontics, Oregon Health and Science University School of Dentistry in partial fulfillment of the requirements for the M. S. degree

Portland, Oregon 97239

December 2009

A thesis presented by Holly J. Grimslid, DMD

In partial fulfillment for the degree of Master of Science in Orthodontics

December 2009

[redacted]

John Mitchell, PhD

Associate Professor

Department of Restorative Dentistry

[redacted]

David A. Covell, Jr., PhD, DDS

Associate Professor and Chairman

Department of Orthodontics

[redacted]

Larry Doyle, DDS

Graduate Program Director

Department of Orthodontics

ABSTRACT

Introduction

Studies have documented the use of titanium mini-implants in providing skeletal anchorage for orthodontic tooth movement. Clinical success rates are variable and typically reported between 70% and 100% . The purpose of this in-vitro study was to test the hypothesis that mini-implants with collars give the orthodontist superior force resistance, superior stability (anchorage) and cause less surface bone strain compared with mini-implants without collars.

Materials and Methods

Thirty titanium alloy mini-implants, 1.5 X 10.5 mm, were placed in bone analogue specimens with cortical bone thicknesses 1.0 mm, 1.5 mm and 2.0 mm (n=10 each), and the maximum insertion torque (MIT) was recorded. Half were mini-implants with collars, half were without collars, and all were subjected to a tangential force loading perpendicular to the mini-implant through a lateral displacement of 1.5 mm. Statistical analyses, consisting of 2 x 3 factorial analysis of variances (ANOVA's) and Tukey's post-hoc testing were used to compare mini-implant collar group mean force-deflection values, yield points, MIT's and slope of the force- deflection curves. Additionally, eight mini-implants were placed in bone analogue specimens with a cortical bone thickness of 2.0 mm. Half were mini-implants with collars, half were without collars, and all were subjected to a similar tangential force through 30N. Electronic speckle pattern interferometry (ESPI) was used to detect surface strain values on the compression side of mini-implants loaded either once or multiple times (n = 4 each). Specific

strain values (με/N), slope of the specific strain–deflection curve and mini-implant displacement were evaluated.

Results

Deflection force values were significantly greater for mini-implants with collars. The slope of the mean anchorage force to displacement curve was significantly greater for mini-implants with collars. Specific strain values were greater for mini-implants loaded multiple times and mini-implant displacement was greater for mini-implants without collars.

Conclusions

Mini-implant collars provide the orthodontist with superior anchorage force resistance, reduced cortical bone stress, and superior stability compared with mini-implants without collars.

TABLE OF CONTENTS

LIST OF TABLES

LIST OF FIGURES

LITERATURE REVIEW

Introduction:

Anchorage control is a desired component for successful orthodontic treatment. Adult cases, periodontally compromised patients and those with reduced dentitions have an even greater need for anchorage. Many case reports have documented the successful use of titanium mini-implants for rigid fixation to provide orthodontic anchorage without patient compliance (Costa et al., 1998; Kuroda et al., 2004; Ohme et al., 2001; Park HS et al., 2001; Park HS et al., 2002). Orthodontic mini-implants have distinct advantages when compared with traditional endosseous implants used as anchors: minimal surgical invasiveness, versatility in placement site, smaller size and relative affordability (Costa et al., 1998; Freudenthaler et al., 2001; Kanomi et al., *1997).*

Because the primary stability of mini-implants is believed to result from mechanical interlock, a waiting period for osseointegration prior to the application of an orthodontic load has been deemed unnecessary (Costa et al., 1998; Melsen B, 2005; Liou et al., 2004). On the other hand, because mini-implants are not osseointegrated, their anchorage potential is most likely influenced by factors associated with primary stability. Essential factors affecting primary stability include the quantity and quality of bone into which the mini-implant is placed, implant design, and insertion modalities (Miyawaki et al., 2003; Huja SS et al., 2005; Brettin et al., 2008).

Mini-implant loss rates, though improving, have been unsatisfactorily high and the probable causes of mini-implant losses are quite variable. A recent systematic review found in human clinical studies that success rates ranged from 70-100% (Janssen et al., 2008). In a retrospective study in 2003, Miyawaki et al., correlated a decrease in mini-implant diameter and high mandibular plane angle with significantly lower success rates. No significant correlation

was found between success rate and screw length, type of placement surgery, immediate loading, age, sex, crowding, anteroposterior jaw base relationship, controlled periodontitits, or temporomandibular joint disorder symptoms. Morarend et al., 2009, mechanically confirmed large-diameter (2.5 mm) mini-implants provide increased anchorage force resistance compared with smaller-diameter (1.5 mm) mini-implants. In a prospective study of risk factors associated with mini-implant failures. In 2004, Cheng et al., reported that both mini-implant length and loads of 100-grams to 200-grams had no significant affect on mini-implant success. This same study also recommended placing mini-implants in keratinized mucosa and to avoid bone overheating when placing mini-implants in dense bone regions. Others, however, found no difference in the success rates of mini-implants placed in keratinized or non-keratinized mucosa (Adell et al., 1981; Albrektsson & Lekholm, 1989). Case reports have also documented problems associated with mini-implant mobility and peri-implant inflammation (Melsen & Costa, 2000; Cheng HC et al., 2003; Cheng SJ et al., 2004). The persistence of variable and higher than ideal mini-implant loss rates suggests there may be factors not completely explored contributing to mini-implant failures.

Some have suggested that there is a relationship between the type of force system used and mini-implant failure. The application of excessive force has been proposed as a probable cause for mini-implant failure, as has the use of a large lever arm when applying an orthodontic load (Buchter et al., 2005; Weichmann et al., 2007). Recently, Brettin et al., 2008, found that bicortical mini-implant placement could provide a force system with superior force resistance, reduced cortical bone stress and greater stability (anchorage) compared with monocortical mini-implant placement. Morarend et al., 2009, supported this finding suggesting that smaller-diameter (1.5 mm) bicortical mini-implants provide anchorage force resistance at least equal to larger- diamteter (2.5 mm) monocortical miniscrews. In addition, studies have revealed a correlation between the strain levels generated at the implant-bone interface and the success rate of miniscrews (Motoyoshi et al., 2005; Buchter et al., 2005; Wiechmann, 2007). Since excessive

bone strain could contribute to bone resorption, mini-implant mobility and early mini-implant loss, examining the relationship between bone strain and the surface area or volume over which an orthodontic load is applied is important.

Electronic speckle pattern interferometry (ESPI) is a non-invasive optical technique used to qualitatively and quantitatively measure deformation and strain typically on the surface of objects. In-plane ESPI evaluates deformation normal to the viewing area of the object. An advantage of ESPI is its extreme sensitivity, which allows detection of displacements as small as tens of nanometers. ESPI is a novel and effective way to evaluate strain in bone analogue adjacent to the mini-implant.

Theoretically, a mini-implant implant collar placed in direct contact with the surrounding cortical bone may be another method used to improve the overall force system. By increasing the surface area and volume of cortical bone over which the orthodontic load is distributed, the mini-implant collar may reduce the strain at the implant-bone interface. The literature lacks any studies examining the mechanical effects of an orthodontic mini-implant collar. The objective of this in-vitro study was to examine the mechanical effects of a mini-implant collar. Specifically, the force resistance of a monocortical mini-implant with a collar was compared with that of an identically designed mini-implant except without a collar and the bone strain patterns in the area of compression adjacent to these monocortical mini-implants were compared

Mini-implant Success Rates:

Variability exists in the overall success rates of mini-implants used for orthodontic treatment. A recent systematic review found in clinical studies success rates for mini-implants ranged from 70-100% (Janssen et al., 2008). Some authors have reported success rates for orthodontic mini-implants of 90% or greater (Chung, 2000; Kim, 2002; Woo, 2003; Park et al., 2006) a figure much improved over the past, yet failures still occur.

There have been many successful treatment results with mini-implants, yet there have been many large clinical studies that have reported success rates less than 90%, which is less than satisfactory for many providers. A study with 44 patients and 140 mini-implants reported a cumulative survival rate of 89% (Cheng, 2004). This was comparable with the cumulative success rate of 87% with 49 patients and 133 mini-implants (Wiechmann et al., 2007). Miyawaki *et al.* found no significant difference between the success rate of miniplates (96.4%) and mini-implants with diameters of 1.5mm (83.9%) and 2.3mm (85.0%) (Miyawaki et al. 2003). In addition, a recent large retrospective study of 480 identical mini-implants found an overall success rate of 83.8% (Moon et al., 2008).

Success rates for orthodontic mini-implants have been improving since their inception, yet large clinical studies continue to report ranges between 80% and 100%. There are factors yet to be considered or not fully explored contributing to the continued variability in mini-implant success rates. The orthodontic mini-implant design characteristic of a collar is one factor that has not been examined in the literature but should be explored.

Cortical Bone Thickness

Both the quantity (bone volume) and quality (bone density) of alveolar bone are important factors for determining the stability of orthodontic mini-implants (Miyawaki et al., 2003). In addition, it has been suggested that cortical bone thickness has an effect on mini-implant success rates (Miyawaki et al., 2003; Motoyoshi et al., 2007). Motoyoshi et al. evaluated the relationships among cortical bone thickness, the inter-root distance, the vertical space, and the success rates of mini-implants for orthodontic anchorage. No relationship was found between the stability after mini-implant placement and the width and height of the bone supporting the mini-implant. The cortical bone thickness was significantly related to the stability

of the mini-implants and placing them in sites with a cortical bone thickness of 1.0 mm or more was recommended to increase success rates (Motoyoshi et al., 2007)

In general, the maxilla has relatively thin cortices while the mandible is composed of thicker cortices. Park et al. (2002) examined the thickness of cortical bone via computed tomography (CT) and found in the maxilla on average the mean cortical bone thickness approached 1.5 mm. In the mandible, the cortical bone thickness was more variable and ranged from a mean of 1.71 mm to 3.17 mm. In the maxilla, the alveolar bone near the posterior, between the premolars and molars, was considered the best site for implantation of mini-implants because of thicker cortical bone when compared to the anterior region and the greater distance between the second premolar root and the first molar root. (Park et al, 2002). The infra-zygomatic crest, usually located above the maxillary first molar, was found to have a cortical bone thickness of 3-4 mm, but was variable depending upon the pneumatization of the maxillary sinus (Liou et al., 2004).

Deguchi et al. (2006) evaluated three-dimensional computed tomographic images (3D) CT from 10 patients and concluded the safest buccal location for mini-implant placement in both the maxilla and mandible was mesial or distal to the first molar, and that an acceptable size for a mini-implant was less than 1.5 mm in diameter and 6 to 8 mm in length. The safest lingual placement site was mesial to the first molar. The average cortical bone thicknesses in the maxilla measured at a level 3 to 4 mm from the gingival margin were 1.8 mm, 1.5 mm, and 1.3 mm mesial and distal to the first molar and distal to the second molar, respectively. Measured at a more apical level (6 to 7 mm from the gingival margin), cortical bone thickness averaged 1.6 mm mesial and distal to the first molar. The averages of lingual cortical bone thickness were 1.7 mm, mesial and distal to the first molar, and distal to the second molars. Significantly more cortical bone thickness was observed on the lingual side only at the site distal to the second molar region. In the premaxilla region, the average cortical bone thickness was 1.4 mm at the A-point level.

In the mandible, at the occlusal level, the averages for cortical bone thickness were 1.9-mm, 2.0-mm, and 1.9-mm, mesial and distal to the first molar, and distal to the second molar, respectively. At the apical level, thicknesses averaged 1.8-mm mesial and distal to the first molar. There was no significant difference between locations in the mandible. A significant difference between jaws, with the mandible being greater, was observed mesial to the first molar and distal to the second molar. Also of note, Deguchi et al. (2006) found no significant difference for sex, age, or side in cortical bone thickness.

Ono et al. (2008) evaluated three-dimensional reconstructed images of bone around the first molars in 39 maxilla and 41 mandibles using dentomaxillofacial limited cone beam CT. The cortical bone thickness was measured from 1.0 mm to 15.0 mm below the alveolar crest at 1.0 mm intervals. The average cortical bone thickness ranged from 1.09 mm to 2.12 mm in the maxilla and 1.59 mm to 3.03 mm in the mandible. The cortical bone of the mandible was significantly thicker than that of the maxilla at any vertical location in cross sections mesial and distal to the first molar. In addition, the greater the height in both arches, the thicker the cortical bone. Unlike Deguchi et al.(2006), the cortical bone was significantly thinner in females than in males in the region of attached gingival in the maxilla mesial to the first molar. Furthermore, this study found significantly less cortical bone thickness at heights of 3-8 mm in the mandible mesial to the first molar in adolescents when compared to adults (Ono et al.,2008).

Technology has advanced our ability to accurately predict the amount of cortical bone at implant sites. Recently, authors have suggested evaluating cortical bone thickness prior to mini-implant placement to make implant selection decisions. For example, it was recommended that in areas of thin cortical bone it may be advantageous to use surface–treated orthodontic mini-implants with high osseointigration potential in order to improve success rates (Kim, 2008). In general, the maxilla has thinner cortical bone with an average near 1.5 mm and the mandible has thicker cortical bone ranging between 1.5 and 3.0 mm. In the current study the use of a bone

analogue with cortical bone thicknesses of 1.0 mm, 1.5 mm and 2.0 mm accurately represents the cortical bone thickness of the human maxilla and mandible.

Bone Quality and Bone Material Properties

Misch's classification system is the most recognized and utilized classification system for bone quality. Misch (1998) classified bone density into four groups – D1, D2, D3 and D4 – based on the number of Hounsfield units (HU). Hounsfield units are units of measurement used in computed tomographic scanning to characterize tissue density. D1 (>1,250 HU) is dense cortical bone primarily found in the anterior mandible, buccal shelf and midpalatal region. D1 bone has the tactile analogue of oak wood. D2 (850-1,200 HU) is porous cortical bone with coarse trabeculae found primarily in the anterior maxilla, the midpalatal region and the posterior mandible. D2 bone has the tactile analogue of pine wood. D3 (350-850 HU) is thin (1.0-mm), porous cortical bone with fine trabeculae, found primarily in the posterior maxilla and mandible. D3 has the tactile analogue of balsa wood. D4 (150-350 HU) is fine trabecular bone with little to no cortical bone, found primarily in the tuberosity region. D4 has the tactile analogue of polystyrene foam (Misch, 1998).

Based on Misch classifications, regions of D1 to D3 bone were considered adequate for mini-implant insertion. In addition, mini-implants placed in D1 bone may require a purchase point to perforate the thick cortical plate. Mini-implants placed in D1 and D2 bone may exhibit lower stress at the screw-bone interface and may provide greater stationary anchorage during loading (Sevinmay et al, 2005). Though the Misch's classification system is the most recognized it lacks specific quantitative values.

Park et al. (2008) evaluated 63 sets of computed tomographic (CT) images to evaluate the density of the alveolar and basal bones of the maxilla and mandible. The highest bone density in the maxilla was observed in the canine and premolar areas, and the maxillary tuberosity showed

the lowest bone density. Density of the cortical bone was greater in the mandible than in the maxilla and showed a progressive increase from the incisor to the retromolar area (Park et al., 2008).

Misch et al. (1999) later quantitatively evaluated the bone density, elastic modulus and ultimate compressive strength of trabecular bone in the human mandible. Nine mandibles were sectioned into three regions bilaterally: Region 1, which included the incisors and canines; Region 2, which included the premolars and Region 3, which included the molars. The density of the mandibular trabecular specimens ranged from 0.85 to 1.53 g/cc^3, with a mean value of 1.14 g/cm^3. With the cortical plates present, the elastic modulus of the trabecular bone ranged from 24.9 to 240 MPa, with a mean value of 96.2 MPa. The ultimate compressive strength of the trabecular bone ranged from 0.22 to 10.44 MPa, with a mean value of 3.9 MPa. In addition, they concluded that the trabecular bone in the human mandible has significantly higher density, elastic modulus and ultimate compressive strength in the anterior region than in either the middle or distal regions. Two types of trabecular bone were defined in a clinical classification scheme for the mandible and maxilla: "coarse" (D_2) in the anterior mandible and "fine" trabecular bone in the posterior mandible (D_3) (Misch et al., 1999).

Seong et al. (2009) examined the physical properties of 4 edentulous maxillas and mandibles using the nano-indentation technique. 200-mm long bone blocks were taken from the anterior and posterior regions of each maxilla and mandible. The overall mean elastic modulus of maxillary and mandibular cortical bone was 17.7 Gpa. The combined apparent density (cortical and trabecular bone) averaged 1.18 g/cm^3 in the mandible and 0.67 g/cm^3 in the maxilla. The combined apparent density was less in the posterior maxilla than any other region. The elastic modulus and hardness, however, were higher in the posterior than they were in the anterior. These findings suggest that the amount of cortical bone and trabecular bone per unit volume available is more important for implant success, than stiffness of the cortical bone or trabelular bone in contact with the implant (Seong et al,.2009).

Dabney and Dechow (2003) reported a density of 1.85 -2.0 g/cm^3 for cortical bone from 10 dentate human mandibular samples. Ultrasonic velocities were used in order to calculate the elastic moduli in three axes. They found the grand mean elastic moduli in three axes of 600 specimens were 22.8 GPa for E_3, 17.0 GPa for E_2 and 12.7 GPa for E_1 (Dabney and Dechow, 2003).

The overall density of bone, or the amount of cortical bone and trabecular bone per unit volume available appears to be more important than the stiffness or moduli of the cortical bone or trabelular bone in contact with the mini-implant. The current study used synthetic cortical bone with a density of 1.64 g/cm^3 and an elastic modulus of 16.7, which is similar to the 1.85-2.0 g/cm^3 density range and 12.7 Gpa to 22.8 Gpa moduli range reported (Dabney and Dechow, 2003). The current study used synthetic trabecular bone with a density of 0.24 g/cm^3 and a modulus of 123 MPa, which was less than the 0.85 to 1.53 g/cm^3 density range and similar to the 24.9 to 240 MPa moduli range reported by Misch et al., with a mean value of 1.14 g/cm^3. Tactilely, the current study used bone that was most closely related to D1 bone.

Immediate Loading

Early studies questioned the legitimacy of immediately loading orthodontic mini-implants. Histologically, it was shown that, when a load is placed before osseointegration, a layer of fibrous tissue would interpose at the bone-implant contacts (Majzoub et al., 1999). This layer of fibrous tissue may allow the miniscrew to be extruded and tipped in the direction of orthodontic loading. It was thought that the fibrous tissue becomes compressed, and then the threads of the mini-implant become mechanically locked into the surrounding bone. This may explain why some mini-implants are displaced but clinically not mobile (Liou et al., 2004). Other investigations indicated that although premature loading has been interpreted as inducing fibrous tissue interposition, immediate loading *per se* was not responsible for fibrous

encapsulation and mini-implant failure. Szmukler-Moncler et al., concluded that it was excess micromotions during the healing phase that interferes with the bone repair process (Szmukler-Moncler et al, 1998). Further experimental observations suggested that micromotions themselves do not systematically lead to fibrous tissue interposition and that tolerance to micromotion is both design and load dependent.

The effects of continuous lateral or oblique load on the peri-implant bone were described *in vitro* using FEA. These models reveal that under conditions of a direct bone/implant contact and moderate load applications, marginal strains are lower than the upper limit of tolerable bone strains. Therefore, immediate implant loading seemed to be possible without impairing implant stability (Mihalko et al., 1992). Furthermore, experimental studies have not been able to demonstrate implant loosening induced by orthodontic load even when these loads were applied immediately (Wehrbein et al., 1997; Akin-Nergiz et al, 1998).

Immediately loading an orthodontic mini-implant is an acceptable protocol today. A waiting period is deemed unnecessary because the primary stability, or mechanical retention, of the mini-implant is sufficient to sustain regular orthodontic loading (Costa, 1998; Melsen, 1999; Wiechmann, 2007). A recent clinical study found that the timing of the loading of 1.3-mm mini-implants was not related to the success rate. They reported a high success rate of 89.9% with 79 immediately loaded mini-implants (Kuroda, 2007). Garfinkle et al. (2008) in a recent clinical study evaluated 82 mini-implants 1.6 mm in diameter and 6mm in length. In each quadrant one mini-implant was loaded with up to 250-g of force and one was unloaded. The 250-g force was either applied immediately or after 3-5 weeks of healing. The overall mini-implant success rate was 70.7% and there was no statistically significant difference between the immediately loaded mini-implants (80.0%) and delayed loaded mini-implants (80.95%). The combined success rate for all loaded mini-implants (80.49%) was significantly higher than that of unloaded mini-implants (60.98%) (Garfinkle et al., 2008).

A number of clinical studies confirmed a positive effect of orthodontic loading on the stability of titanium screw implants, as well as the effects on peri-implant bone (Roberts et al., 1994; Wehrbein et al., 1993; Hurzeler et al., 1998). Romanos et al. (2002) ultimately showed that immediate loading may actually increase the ossification of the alveolar bone around the implant. Therefore, they postulated that immediate loading might actually contribute to the good prognosis of orthodontic mini-implants (Romanos et al., 2002). Serra et al. (2008) histologically supported the notion that biomechanical stimulation induces acceleration of bone healing by finding there was less fibrous tissue and more remodeling in an immediately loaded implant group at 4 weeks when compared to an unloaded implant group at 4 weeks. After 12 weeks, however, they found high remodeling but less mineralized bone formation around the loaded implants when compared to the unloaded group (Serra, 2008). Potentially, the mineralization or quality of the bone formed when immediately loaded is different when compared to that formed when the load application is delayed.

To date, research shows that immediately loading does not compromise orthodontic mini-implant success rates. As a result, most mini-implants placed today are loaded immediately. The bone strain that results when a mini-implant is immediately loaded are dependent on the load, the surrounding bone characteristics and the mini-implant characteristics. The interaction of these variables and how this relates to mini-implant success are areas that need further exploration.

Strain and Bone Response – General

Mechanical stress causes strain in bone tissue. Stress is defined as force per unit area. It has the same units of pressure, however it is a much more complex quantity than pressure because it varies both with direction and with the surface it acts on. Strain is defined as the amount of deformation, whether shortening or lengthening, an object experiences compared to its original size and shape. For example, if a block 10 cm on a side is deformed so that it becomes 9

cm long, the strain is 1/10 or 0.1. This is sometimes expressed as a percent but strain is dimensionless.

The degree of strain correlates with stress and the mechanical characteristics of bone. According to Frost, the amount of strain can be divided into various ranges, permitting us to predict the effects on the bone (Frost, 2004). The lower limit of the bone's equilibrium occurs at 50 to 100 μStrain. At this load range, due to continuous bone remodeling, as much bone tissue is formed as is resorbed. Below this limit, due to under-use bone is resorbed. The upper limit of bone's equilibrium is 1,000 to 1,500 μStrain. Bone formation is the initial response above this limit. Additional strain, however, leads to microfissures and microfractures in the bone tissue. At 3,000 μStrain the ongoing repair process is surpassed and bone resorption occurs. At strain levels above 25,000 μStrain macroscopic bone fractures occur.

Wolff's law is a hypothesis that the mechanical environment directly influences the structure and strength of bone. Wolff's assumption is that cortical bone is simply more dense trabecular bone. This assumption probably is not accurate as if this were true, cortical and trabecular bones should have exactly the same elastic properties.

Garfinkle et al. reported that combined success rates for all loaded mini-implants (80.49%), both immediately and delayed loaded, were significantly higher than those of unloaded mini-implants (60.98%) (Garfinkle et al., 2008). This finding supports the idea that without physiologically tolerable bone strain levels occurring at the implant-bone interface bone resorption and potentially mini-implant failure may occur. Understanding bone biology combined with the ability to predict strain at the bone-implant interface accurately may help us better understand mini-implant loosening and predict mini-implant failures.

Bone Response Orthodontic Mini-implant

The amount of bone stresses and strains are dependent on the geometry of the screw as well as the mechanical properties of the implant and bone. Buchter et al. (2004) found

differences in implant stability between implant systems and suggested that this may be based on the differences in implant geometry influencing the stress and strain distribution in peri-implant bone (Buchter et al, 2004). Buchter et al. (2005) later concluded that moderate static, lateral loading of mini-implants with forces typically used for orthodontic movement, does not impair implant stability. However, in a later study they stated that above a defined threshold marginal bone strains cannot be tolerated by the bone tissue, leading to implant loosening (Buchter et al., 2005).

Development and maintenance of rigid implant fixation during a period of orthodontic loading is essential for effective treatment. Secure fixation can be compromised by significant peri-implant bone loss. Liou et al. (2004) reported that mini-implants under orthodontic load were tipped to the pressure side and suggested this may cause interposition of the fibrous tissue between the mini-implant and bone. They hypothesized that initial bone remodeling on the upper end of the pressure side of the mini-implant may be harmful to the stability of the mini-implant. (Liou et al., 2004). Crestal peri-implant bone loss can be the result of a number of factors, including biomechanical factors: high localized stresses can cause bone microfracture and subsequent resorption, while abnormally low stresses related to implant-related stress protection can lead to atrophy (Pillar et al., 2005). The goal may be to establish a more osteogenic stress state at the implant-bone interface in accordance with Carter's tissue differentiation hypothesis (Carter et al., 1998)

It is generally accepted that peri-implant tissue formation and mineralization by osteoblasts are dependent on the local mechanical environment at the bone-implant interface (Szmukler-Moncler et al.,1998). Frost and colleagues suggested that proliferation and differentiation of the osteoblasts responsible for peri-implant tissue formation are regulated by the local mechanical environment. This relationship of defined cell deformation and bone remodeling has been documented in various in vivo studies. Loading of intact bone after osteotomy, during growth, in fracture healing, and during distraction osteogenesis resulted in

strain related tissue responses (Cheal et al., 1991; Meyer et al., 1999). Whereas physiological bone loading (500-3000 μstrains) leads to mature bone formation, higher peak strains result in immature bone mineral formation and fibroblastic cell pattern. Additionally, the finite element analysis (FEA) calculations of Isidor et al. (1997) revealed that not all forces may be tolerated by the crestal bone on a long-term basis. They reported that high strain values above 6700 μStrain resulted in peri-implant bone resorption and a negative balance between bone apposition and bone resorption (Isidor, 1997).

As the local mechanical environment around implants is dependent on the forces imposed and the implant/bone surface interaction, certain implant designs may promote osseointegration by providing a favorable local mechanical environment for bone formation (Simmons et al., 2001). Based on this reasoning, it was assumed that the undisturbed osseointegration process observed also with loaded implants was the result of the macro design with its characteristic three-dimensional form, providing a local mechanical environment in the early interfacial tissue that prevented peak strains at the interfacial layer (Simmons et al., 2001).

Although a typical orthodontic force from 100 to 300 g is lower than occlusal force, the stress applied to bone tissue around the mini-implant in a small area may be concentrated and as high at 33 MPa (Motoyoshi et al., 2005). The stress transmitted to the bone surrounding the orthodontic mini-implant is dependent on the surface area in contact with the surrounding bone. Stress may be excessive because the mini-implant has a smaller surface area which may induce more bone resorption than apposition around the mini-implant. Previous studies reveal a strong correlation between the strain levels generated at the implant-bone interface and the success rate of the implant (Motoyoshi et al., 2005; Buchter et al., 2005; Wiechmann, 2007). Stresses above optimal levels may result in localized bone microfracture, followed by ischemia and necrosis while stresses below optimal levels may result in initial instability and bone resorption causing further micromotion. Both scenarios lead to strain associated implant failure.

Fritz et al. (2003) examined the histomorphologic effects of orthodontic loading in an animal model. They evaluated 16 cylindrical acid etched miniscrews placed in foxhounds and loaded after a six month healing period. 8 miniscrews were loaded with a 50 cN extrusive force while 8 were loaded with a 200 cN translatory force. They examined the apical, intermediate and marginal areas surrounding the implant. The peri-implant bone activity was documented by polychrome sequential labeling. The osteodynamic process was visualized by injecting various fluorescent dyes with calcium affinity at different timepoints. The qualitative assessment was based on the classification of Wehrbein et al. (1993) with reference to apposition lines identifiable by fluorescent microscopy. Appositional adaptation was classified as new formation of bony matrix and was differentiated from mature remodeling within existing osseous structures.

Histomorphometric analysis revealed differences in the osteodynamics at the bone-implant interface. Due to elastic deformation, extrusive loading induced increased appositional activity, primarily in the marginal and intermediate implant areas. Translatory loading led to less pronounced and more evenly distributed appositional activity. In addition, after extrusive loading the extent of peri-implant remodeling activity was found up to 980 μm from the implant body. This was found in all three vertical areas analyzed. After translatory remodeling, however, a shorter remodeling range of between 300-700 μm loading was found with the highest ranges found in the cervical and apical regions. The extent of cervical inflammatory bone destruction was also evaluated in reference to the lower edge of the implant neck. The mean distance between the alveolar margin and implant neck was -0.12 +/- 0.41 with extrusive loading and -0.75 +/- 1.35 with translatory loading (Fritz et al., 2003). This indicates more cervical bone resorption was found with translatory loading likely due to excessive bone strain at the cervical margin.

The amount of bone stress and strain have been widely documented to be dependent on the geometry of the screw as well as the mechanical properties of both the implant and bone. The

mini-implant design characteristic of a collar may help minimize areas of excessive bone strain and therefore minimize bone resorption and mini-implant failures. A mini-implant collar theoretically may minimize bone strain at the cervical margin of the mini-implant neck upon translatory loading.

Mini-Implant Failure

Endosseous implants rely on osseointegration for stability and most long-term clinical studies attributed failures to overloading or excessive loading when no peri-implantitis was present. Most of the endosseous implant losses were considered to be the result of excessive strains and stresses at the bone/implant interface (Adell et al., 1981). Without reliance upon osseointegration it is the orthodontic mini-implants primary stability, or initial stability, that appears most important for mini-implant success. Factors such as bone quality, bone quantity and implant design become more significant. Melsen & Verna found orthodontic mini-implant failures often occur because of placement in regions of low bone density and inadequate cortical bone thickness (Melsen & Verna, 2005). Other authors have also concluded that bone quantity seems to be a major factor in the stability and success of mini-implants (Costa, 1998; Miyawaki, 2003).

Buchter et al. in an animal model demonstrated mini-implant failure was directly related to the tipping moment (TM) at the bone rim. TM (Nmm) = force (N) x lever arm length (mm). By reducing the main TM under a threshold of 900 cNmm (300cN and 3mm lever arm) mini-implants could be loaded immediately without impairment of implant stability and implant success rates (Buchter, 2005). This is in agreement with earlier studies demonstrating that implants remain stable when subjected to tip forces ranging from 100 to 300 cN (Roberts et al., 1989; Roberts et al. 1994).

More recently, Wilmes et al. recognized that there are issues other than primary stability to consider, such as magnitude of applied forces and torques, the soft tissue thickness, oral hygiene, smoking habits, and patient age. Each may exert a relevant influence on the stability and survival rates of an orthodontic implant (Wilmes et al., 2008).

Despite the recent surge of orthodontic mini-implant research, many authors have concluded that it still remains questionable as to which factors affect loss rates, and how relevant these factors are (Miyawaki et al., 2003; Cheng et al., 2004; Fritz et al., 2004; Berens et al., 2005). Clearly there is a relationship between the quantity and quality of the host bone in the placement site and the implant form. This relationship is fundamental to determining the maximum force that can be supported as all factors ultimately affect bone strain levels.

Orthodontic Forces Placed on Mini-implants

Forces placed on mini-implants can vary widely and typical orthodontic loads are approximately 0.3 to 4 N, or roughly 30 to 400 grams, depending on the desired tooth movement (Ren et al., 2003). Case studies have reported that mini-implants loaded from 70 to 200 g are required for tooth translation (Park HS et al., 2002) and 150 g for intrusion (Park YC et al., 2003). Huja et al. (2005) demonstrated that mini-implants could withstand significantly greater force levels than needed for tooth movement when loaded purely in the axial direction; they observed maximal force loads of 388.3 N. However, axial loading does not mimic the direction of orthodontic forces (Huja et al., 2005).

A recent systematic review found no differences in success rates of orthodontic mini-implants related to the amount of force applied when the range was between 100-400 grams (Janssen et al., 2008). This is in agreement with earlier studies demonstrating that implants remain stable when subjected to tip forces ranging from 1 to 3N (Roberts et al., 1989; Roberts et al. 1994). In addition, the typical orthodontic force of 100 to 400 grams applied to a mini-

implant will not cause failure in most cases given the 80% to 100% success rates reported today in orthodontic literature.

Forces in the range of 50 to 400 grams are adequate to accomplish most orthodontic movements. Mini-implant success rates remain similar if forces applied to mini-implants are kept in the range of 100-400 grams. Mini-implant success rates continue to be less than ideal and the possibility that orthodontic forces could produce excessively high localized bone strain surrounding mini-implants requires further research.

Mini-implants and Bone Strain - FEM

Finite element method (FEM) is a powerful technique originally developed for numerical solution of complex problems in structural mechanics, and it remains the method of choice for complex systems. In the FEM, the structural system is modeled by a set of appropriate finite elements interconnected at points called nodes. Elements may have physical properties such as thickness, coefficient of thermal expansion, density, elastic modulus, shear modulus and Poisson's ratio. This method has also recently been used to investigate how mini-implants interact with surrounding bone.

Melsen et al. (2005) developed two different three-dimensional finite element models (FEM) to evaluate the load transfer from mini-implant to surrounding bone. A geometrically accurate model and a parametric model were created. The parametric model evaluated the influence of both the cortical thickness and the underlying trabecular bone density. A mesially directed perpendicular force of 50 g was applied to the head of the mini-implant. The force level of 50 g at the start of treatment was chosen from the results of a previous FEM analysis (Dalstra et al., 2004). Under this loading condition, the mini-implant is displaced in a tipping mode, causing tensile stress in the direction of the force. Stress levels were higher in the cortical bone

than in the underlying trabecular bone; the opposite was the case for the strain values. Although a peak value of 2465 microstrain was reached in the trabecular bone the average magnitude for bone strain was 10 to 100 microstrain. The parametric model revealed that the thickness of the cortical bone determines the overall load transfer from the mini-implant to bone and that the stiffness (or modulus) of the trabecular bone plays only a minor role. When evaluating the peak strains occurring in bone relative to the bone strains according to Frost's mechanostatic theory, it becomes apparent that bone strains can reach values associated with the pathological overload window only for thin cortical bone (<0.5 mm) with low-density trabecular bone (Frost, 1994). For medium- and high-density trabecular bone this danger is not present, since the bone strains always occur within the mild overload or adapted windows (Melsen et al., *2005).*

Stahl et al. later tested 16 mini-implants using (FEM) to quantify implant deflection, bone stress and bone strain around mini-implants. A 5 N load was applied and the variables evaluated were cortical bone thickness (1.0 and 2.0 mm) and Young's modulus of cancellous bone (100 MPa and 1 GPa). They determined that cortical bone thickness was a decisive factor in the biomechanical behavior of mini-implants. Regardless of which Young's modulus of cancellous bone was applied, the mini-implants deflection, stress and strain in the surrounding bone tissue was reduced as the cortical bone thickness increased. In addition, the thinner the cortical bone was the more influential the Young's modulus of the cancellous bone became. The most unfavorable combination was thin cortical bone (1.0 mm) and the smallest Young's modulus (100 MPa). These conditions led to the highest stress and stain levels in the cortical bone (Stahl et al., 2009).

Stahl et al. (2009) also noted that doubling the cortical bone thickness from 1.0 mm to 2.0 mm reduced the median of the implant deflections by 32% for a Young's modulus of cancellous bone of 100 MPa. The deflections ranged between 2.1μm to 19.6 μm with a median of 6.1μm. (.006 mm) Variation in the Young's modulus of cancellous bone between 100 MPa and 700 MPa

did not affect the deflection's median with cortical bone 2.0 mm thick. Only a tenfold increase to 1 GPa reduced the median by 8% to 5.6 μm.

The greatest stress was also obtained in 1.0 mm thick cortical bone in conjunction with cancellous bone and a Young's modulus of 100 MPa. The stress in the cortical bone ranged from 26 MPa to 186 MPa with a median of 64 MPa. Quadrupling the Young's modulus of cancellous bone (400 MPa) decreased the median stress by 25%. Increasing the Young's modulus to 700 MPa decreased the stress in the cortical bone by 27%. The stress in 2.0 mm thick cortical bone was not reduced with a fourfold or sevenfold increase in the Young's modulus of cancellous bone.

The strain, which represents a measure of the relative change in length are given in the unit μStrain. A change in the length of one percent corresponds to one hundreth of a unit of strain, or 10,000 μStrain. The greatest strain values were found utilizing a cortical bone thickness of 1.0 mm and cancellous bone with a Young's modulus of 100 MPa. Over 25% of their simulations exceeded the fracture limit of 25,000 μStrain (Stahl et al., 2009).

Stahl et al. (2009) also evaluated the angle of the load application and found that strain is reduced when the implant load direction inclines at an angle up to 45 degrees in the buccal direction. This contradicts the recommendation by some manufacturers to load the mini-implants at 90 degree angles.

Stahl et al. (2009) recognized that the deflection magnitudes they found were low when compared to previous cephalometric studies after therapy with mini-implants (Liou, 2004). This was explained by recognizing that additional factors such as insertion technique, insertion location, oral hygiene and others that can not be simulated by FEM must play a role (Stahl et al., 2009).

There is a clear need to better understand and quantify bone strain occurring adjacent to loaded mini-implants. Current research does not appear to be in agreement on whether it is possible or likely to overload bone with typical orthodontic loads. Having an accurate

understanding of bone strain and knowledge regarding the exact properties of the bone in which mini-implants are placed should help us more accurately predict failures.

ESPI:

Electronic Speckle Pattern Interferometry (ESPI) is currently one of the most advanced optical methods using laser radiation in experimental mechanics. ESPI is a non-invasive technique that uses laser light, together with video detection, recording and processing to visualize static and dynamic displacements of components with optically rough surfaces (Jones & Wykes, 1989). All ESPI configurations rely on the intensity interference of speckle patterns as the basis of measurement. Speckle is the granular-looking interference pattern that occurs when coherent light is scattered off an object. The scattered light waves superimpose, interfering with each other resulting in speckle patterns of light and dark spots. Each speckle is formed by light that is reflected from an area approximately 10 x 10 μm^2 on the surface and its phase, amplitude and intensity are directly related to the microstructure of that area of the object.

The component under investigation must have an optically rough surface so that when it is illuminated by an expanded laser beam the image formed is a subjective speckle pattern. Two light fields are superimposed on the video camera image (different configurations enable different measurements to be made). The two light fields interfere and the resulting light field has random amplitude, phase and intensity, and is therefore also a speckle pattern. If the object is displaced or deformed, the distance between object and image will change, and hence the phase of the image speckle pattern will change. The relative phases of reference and object beam change, and therefore the intensities of the combined light field changes. However, if the phase change of the object light field is a multiple of 2π, the relative phases of the two light fields will be unchanged, and the intensity of the overall image will also be unchanged.

In-plane ESPI illuminates an object by two light fields derived from the same laser beam and incident on the object from opposite sides. When the object is displaced or deformed in the direction normal to the viewing direction (i.e. in its own plane), the phase of one beam increases while the phase of another decreases, so that the relative phases of the two beams changes. When this change is a multiple of 2π, the speckle pattern remains the same, while elsewhere it changes. Fringes obtained by this method represent in-plane displacement contours (Jones & Wykes, 1989).

To visualize this effect, the two beams are combined on a video camera and recorded. When the object has been displaced/deformed, the intensity of each pixel in the reference image is subtracted from the intensity of the same pixel of the deformed sample. The resulting image is a speckle pattern with black 'fringes' representing contours of constant $2n\pi$. The difference between patterns of images taken before and after applying the load are used to detect shifts in the phases of speckles (for a full description, see Jones and Wykes, 1989). Depending on the ESPI configuration these phase shifts correspond to displacements of the surface along one axis (X, Y, or Z in space) and their extent can be determined using a phase shifting algorithm combined with phase unwrapping (Ried, 1986). In the current study we analyzed displacement along the horizontal x-axis, or the direction of the applied axial load. This coincides with the long axis of the samples (Zalansky, 2006).

By using the ESPI approach, it is possible to simultaneously track uni-axial displacements of many points (>10,000) situated along and across the deforming surface. The deformation is represented by a fringe pattern when the image of the deformed sample is analyzed against the undeformed reference image. The resulting image is a speckle pattern with black 'fringes' representing contours of constant 2π. One of the main advantages of this method is its extreme sensitivity, which allows detection of displacements as small as tens of nanometers. The limit of detection is $\lambda/30$, where λ is the wavelength of the laser light. Typically this limit is several hundreds of nanometers (Shahar, 2007).

ESPI is a sensitive, non-invasive optical method that generates specific quantitative measurements for strain. Excessive strain in bone surrounding orthodontic mini-implants may play a role in mini-implant failure or loosening. Understanding and quantifying the strain in the bone adjacent to loaded mini-implants is valuable information and may provide helpful information regarding implant site selection and mini-implant type selection.

ESPI In Dental Research:

Yap et al. (2004) , used ESPI to characterize the modulus of resin-based filling materials. Five light cure composites were tested using two focus region lengths (22 mm; 11 mm) and the modulus (n = 7) was computed based on cantilever beam equations. Data was compared to those obtained from the more common three-point-bend flexural testing (n = 7) based on ISO4049:2000 specifications [ISO]. The correlation between the two ESPI test methods and the ISO three-point-bending test was significant and strong (r =0.94). This is significant in that ESPI may be a viable method of characterizing the modulus of resin based filling materials. Because ESPI is a non-destructive test, time-dependent effects of composites can be determined using the same specimens, which is more efficient and cost effective.

Zalansky et al. (2004) studied the 200-300 μm soft zone of dentin, found beneath enamel in crowns of human teeth. This structurally graded zone is known to be softer when tested for micro-hardness. It also undergoes greater strain compared to bulk dentin, when measured using moiré interferometry. They investigated the deformation and stiffness of this zone by means of ESPI, and nanometer-scale deformations were tracked during compression testing under water. They reported a significantly reduced stiffness of this zone compared to bulk dentin, with mid-buccal regions of teeth averaging 3.5 GPa compared with 9.7 GPa in mid-lingual regions. This supported their hypothesis that the durability of the whole tooth relies upon a bucco-lingual

asymmetric matching of stiffness by means of a cushioning soft layer between enamel and bulk dentin.

Kishen et al. (2004) looked at the thermally induced deformation in human dentin by ESPI. Specimens were prepared from freshly extracted lower central incisor teeth and were mounted on a thermal block to apply thermal loads from room temperature (25°C) to 60°C. The real time speckle patterns were acquired and the digital fringe patterns were subjected to further image processing. The out-of-plane deformations were observed in the plane perpendicular to the long axis of the tooth, while the in-plane deformations occurred in the plane parallel to the long axis of the tooth. The ESPI analysis revealed whole field and distinct thermal responses in human dentin both in-plane and out-of-plane.

Bouillaquet et al. (2006) used EPSI to measure tooth deformation in response to polymerization of five resin composites with a range of polymerization shrinkage. Standardized MOD cavities were prepared and placed in the ESPI apparatus before they were filled with composite (n=10). Their hypothesis was that composites with higher polymerization shrinkage should cause more cuspal strain. They found that the correlation between polymerization shrinkage of the resins and ESPI measured tooth deformation was not straight-forward. Flowable composite did not deform the tooth significantly more than a conventional hybrid composite. Further, an experimental silorane material (with lowest axial shrinkage) induced the least tooth deformation. They concluded that ESPI is a viable method for assessing cuspal strain induced by shrinkage, but that polymerization shrinkage data may overestimate shrinkage-induced tooth deformation. The rate of polymerization shrinkage appeared to mediate the development of cuspal strain.

ESPI is an optical technique that has been widely used in the aerospace industry and civil engineering. It has sparingly been used in dental research but offers many advantages. ESPI is a non-destructive, efficient and highly specific way to evaluate strain in materials. The potential negatives to this technology are cost and having the technological expertise to support it.

Evaluating strain in bone surrounding mini-implants with ESPI provides quantitative information regarding strain distribution which is valuable information which ideally may lead to improved success rates.

Objectives of the Current Study

The purpose of this study is to compare the effects of a mini-implant collar on orthodontic anchorage. Specific objectives include: (1) Compare the force needed for mini-implant displacements of 0.5 mm, 1.0 mm and 1.5 mm in three cortical bone thicknesses (1.0 mm, 1.5 mm and 2.0 mm). (2) Compare the force to yield point in three cortical bone thicknesses (1.0 mm, 1.5 mm and 2.0 mm). (3) Compare the maximum insertion torque (MIT) values. (4) Compare the slopes of the respective force to displacement curves. (5) Compare the bone analogue strain values on the compression side of mini-implants 2.0 mm from the mini-implant head in 2.0 mm cortical bone using ESPI. (6) Compare the slopes of the respective specific strain to distance from mini-implant head curves in 2.0 mm cortical bone using ESPI. (7) Compare the mini-implant head displacement in 2.0 mm cortical bone.

HYPOTHESIS

Hypothesis 1: When applying a force perpendicularly to mini-implants secured in a bone analogue of three cortical bone thicknesses (1.0 mm, 1.5 mm and 2.0 mm), the mean anchorage force resistance for mini-implant displacements of 0.5 mm, 1.0 mm and 1.5 mm will be significantly greater for mini-implant groups with collars than the mini-implant groups without collars.

Null Hypothesis 1: When applying a force, there will be no significant difference in mean anchorage force resistance for mini-implant displacements of 0.5 mm, 1.0 mm and 1.5 mm between mini-implant groups.

Hypothesis 2: When applying a force perpendicularly to mini-implants secured in a bone analogue of three cortical bone thicknesses (1.0 mm, 1.5 mm and 2.0 mm), the mini-implant groups with collars will exhibit significantly higher yield points than the mini-implant groups without collars.

Null hypothesis 2: When applying a force, there will be no significant differences in yield points between mini-implant groups in three cortical bone thicknesses (1.0 mm, 1.5 mm and 2.0 mm).

Hypothesis 3: When inserting the mini-implants into a bone analogue of three cortical bone thicknesses (1.0 mm, 1.5 mm and 2.0 mm), the maximum insertion torque (MIT) will not be significantly different between mini-implant groups with collars and the mini-implant groups without collars.

Null Hypothesis 3: When inserting the mini-implants into a bone analogue of three cortical bone thicknesses (1.0 mm, 1.5 mm and 2.0 mm), the maximum insertion torque (MIT) will be significantly different between mini-implant groups.

Hypothesis 4: When applying a force perpendicularly to mini-implants secured in a bone analogue of three cortical bone thicknesses (1.0 mm, 1.5 mm and 2.0 mm), the slope of the mean anchorage force resistance displacement curves of mini-implant groups with collars will be significantly greater than the mini-implant groups without collars.

Null Hypothesis 4: When applying a force, there will be no significant difference in the slope of the mean anchorage force resistance displacement curves between mini-implant groups.

Hypothesis 5: When applying a force perpendicularly to mini-implants secured in a bone analogue with a cortical bone thickness of 2.0 mm, the strain on the compression side 2.0 mm from the mini-implant head measured with ESPI will be significantly less in mini-implant groups with collars than the mini-implant groups without collars.

Null Hypothesis 5: When applying a force, there will be no significant difference in strain values measured with ESPI between mini-implant groups.

Hypothesis 6: When applying a force perpendicularly to mini-implants secured in a bone analogue with a cortical bone thickness of 2.0 mm, the slopes of the respective specific strain to distance from mini-implant head curves using ESPI will be significantly less for mini-implant groups with collars than the mini-implant groups without collars.

Null Hypothesis 6: When applying a force, there will be no significant difference in the slope of the specific strain to distance from mini-implant head curves between mini-implant groups.

Hypothesis 7: When applying a force perpendicularly to mini-implants secured in a bone analogue with a cortical bone thickness of 2.0 mm, the displacement of the mini-implant head using ESPI will be significantly less for mini-implant groups with collars than the mini-implant groups without collars.

Null Hypothesis 7: When applying a force, there will be no significant difference in the displacement of the mini-implant head.

Hypothesis 8: When applying a force multiple times perpendicularly to mini-implants secured in a bone analogue with a cortical bone thickness of 2.0 mm, the specific strain on the compression side 2.0 mm from the mini-implant head and displacement of the mini-implant head will be significantly greater than when the force was applied once only.

Null Hypothesis 8: When applying a force, there will be no significant difference in the specific strain or mini-implant head displacement.

MATERIALS AND METHODS

Mechanical Loading

Thirty orthodontic mini-implants, n=15 with collars (C) and n=15 without collars (NC) were obtained from the manufacturer (Orthodontic TAADS, Memphis, TN; see Figure 1). These mini-implants were from a single manufactured batch. The collar is the portion of the mini-implant that directly abuts the cortical bone when the mini-implant is fully seated. The collar is 1.0 mm high with a diameter of 3.5 mm. In the collar group (C), the mini-implants were used as provided by the manufacturer. In the non-collar group (NC), the mini-implant collar was milled off by the manufacturer to provide the original implant body diameter of 1.5 mm prior to testing.

The mini-implants were inserted into bone block samples (SAWBONES, Pacific Research Laboratories Inc, Vashon Island, WA, USA). The bone block consisted of two components. One component, made of E-glass-filled epoxy sheets with a density of 1.64 g/cc and a compressive modulus of 16.7 GPa was used as an analog of cortical bone. The other compontent, made of solid rigid polyurethane foam with a density of 0.24 g/cc and a compressive modulus of 123 MPa was used as a cancellous bone analogue (see Table 1). Three experimental bone groups were tested, based on the thickness of the cortical bone analogue: 1.0 mm, 1.5 mm and 2.0 mm (n=10 each).

Samples were cut from experimental bone blocks having final dimensions 120 mm (L) x 11.5 mm (W) x 13.5 mm (D). Each implant was placed 25 mm from one end and centered in the experimental bone block. To facilitate implant insertion perpendicular to the artificial bone block the miniscrews were inserted 3.0 mm via a hand turned drill press (Shop-Task, Model 1720 XM Gold Series, USA) fitted with implant specific driver fittings provided by the implant manufacturer (Orthodontic TAADS, Memphis, TN). After partial mini-implant insertion, the implant driver was attached to a digital torque gauge (Chatillion Digital Torque Gauge, Model DTG, AMETEK, Largo, FL) to complete implant insertion. Each implant was inserted 7.0 mm

deep to the insertion point (IP), regardless of the presence of a mini-implant collar. The maximum insertion torque (MIT) of each implant was recorded (see Table 4). Care was taken to insert the mini-implants with collars to the point at which the collar was touching the bone surface but not engaging the collar into the bone surface to the point of causing significantly higher insertion torques when compared with non-collared implants. All implants were inserted so that the moment arm length was within 0.1 mm tolerance of each other.

Each bone block was placed in a 150 mm (L) x 25 mm (W) x 25 mm (D) custom metal apparatus designed to mount into a Q-test mechanical testing machine (Qtest, MTS systems corporation, Eden Prairie, MN; see Figure 2). Circular openings of 12.75 mm were incorporated into the carrier base and a 12.70 mm diameter steel rod was placed through the holes to secure the sample to the base of the Q-test machine so that the applied load would be parallel to the long axis of the bone sample. The carrier also functioned to prevent moment deformation of the bone block during force application to the mini-implant (see Figure 3). The load was applied with a steel jig affixed directly to the implant using a 1000 lb load cell (MTS systems corporation, Eden Prairie, MN). The jig was used to apply a tangential load to the implant at the force application point (FAP), which was 2.5 mm plus or minus 0.05 mm from the mini-implant insertion point (IP). This coincides with the point where force would be applied to this mini-implant clinically (see Figure 4). Using the Q-test instrument, each mini-implant was subjected to a tangential force load perpendicular to the screw but parallel to the experimental bone block. The crosshead speed was set at 1.0 mm per minute. During loading, displacement of each mini-implant was measured to a maximum displacement of 1.5 mm. Data was collected and recorded electronically.

The following data points were determined: Anchorage force resistance at crosshead displacement .5 mm; Anchorage force resistance at crosshead displacement 1.0 mm; Anchorage

force resistance at crosshead displacement of 1.5 mm; Yield point load; Maximum insertion torque (MIT) and slope of the loading pattern during deformation (see Tables 3 and 4).

ESPI Testing

Specimen Preparation

For these experiments only the 2.0 mm cortical bone thickness was tested, (n=8). Two experimental bone blocks having final dimensions 120 mm (L) x 50 mm (W) x 13.5 mm (D) were cut. A custom metal carrier with base dimensions 177-mm (L) x 127-mm (W) X 12-mm (H) was fabricated. Six 7.0-mm round holes were machined in the carrier base. A custom steel well with dimensions 120-mm (L) x 50-mm (W) x 24-mm (H) was soldered to the carrier base to support the bone block. The bone block was embedded in lab stone (Microstone, Whip Mix Corporation, Louisville, KY) to the level of the cortical bone. The stone was used to rigidly support the experimental bone and isolate deformation to the area around the implant during loading (see Figure 4). The carrier base was rigidly fixed to an adjustable vertical stage with six 7.0-mm diameter bolts. The stage was then rigidly fixed to the optics table. The carrier base was fixed to the optics table so that the surface of the bone was perpendicular to the imaging axis of the CCD camera (see Figure 5).

Additional mini-implants, four with and four without collars were inserted into the experimental bone blocks. Two rows of two implants were inserted into each experimental bone block, one row with collars and one without collars. Multiple implants were placed in each cortical bone sample to insure consistency with implant insertion and eliminate variability, which may occur during changeover of samples. The implants were placed with spacing of 40 mm between implants and from the ends of the block in the long axis and 16.5 mm between implants and from the edges of the block in the short axis. The size of the sample and spacing of the implants was chosen based on pilot studies to eliminate interferences caused by overlapping

strains due to improper placement of miniscrews. Mini-implants were inserted as previously described. Two groups were formed based upon the number of times they were loaded. One mini-implant load group was loaded only initially and another was loaded multiple times (n=4 each).

Experimental set-up

(ESPI) was used to measure strain resulting from loading of implants with and without collars. In-plane ESPI measurements evaluate deformation in the plane of the object surface and were used to quantify strain on the compression side of the loaded implants (see figure 6). A single mode diode laser (Melles Griot, 25-LHP-928-249, Carlsbad, CA) of 35 mW output power with an emission wavelength of 633 nm HeNe was used to illuminate the object. The two illumination ports were made to incident obliquely on the surface of the specimen. The implants were positioned in the center of the point at which the beams converged, which had a diameter of 60.0 mm. The mini-implant was placed at the same height from the isolation table (12.1 mm) and at the same distance from the beam splitter (59.0 cm) to aid in superimposing both images on the CCD camera. An 8-bit Charged Couple Device (CCD) camera with a spatial resolution of 1600 x 1200 pixels, interfaced to a digital computer formed the imaging system. Loading was accomplished by looping 0.016 nickel guitar string (First Act, Boston MA) around the head of the implant at the level of the ligature hole (see figure 5). The string was attached to a 50.0 lb load cell (Interface, model MB-50, Scottsdale, AZ) which was mounted to the motorized stage designed to move the load cell, generating loading of the implant. The height of the loading device was adjusted with force application at the 12.1 mm level.

For these in-plane displacement experiments, the two illumination ports were made to incident obliquely. The intensities of the beams as well as the angles of incidence (11 degrees) were kept equal. The laser illuminated sample was imaged on the CCD plane and real time deformation fringes were displayed on the display monitor (Kishen et al.,2001).

A series of experiments were carried out to measure the real-time deformations of the bone analogue, during which the load applied to the mini-implants was increased from 0.0 to 30.0 Newtons. The speckle patterns were recorded in subtraction mode.

Digital Signal Acquisition

The fringe formation in ESPI is based on intensity correlation. Therefore a process of digital signal subtraction was employed during fringe acquisition. In the digital signal subtraction process, the CCD camera signal corresponding to the speckle pattern of the undisplaced object was stored electronically (carrier fringes). The object was then displaced (after mini-implant loading) and the real time digital signal as detected by the CCD camera was subtracted from the previously stored image. This subtracted signal was high pass filtered, rectified and displayed on a computer monitor where real-time correlation fringes were observed (Murukeshan et al., 1996).

Digital Speckle Fringe Processing

ESPI as with any interferometric experiment produces dark and bright bands of light called fringes. Qualitative and quantitative information is can be gleaned from these fringes. Closely packed fringes indicate a higher displacement gradient with a magnitude inversely proportional to the fringe spacing. The experimental set-up determines the component of deformation represented by the fringes.

An image was first taken of the mini-implant and a millimeter ruler to correlate pixel size with millimeter measurements. See Figure 13 for a representative image. A chart was then created that plotted load (N) versus time (seconds). This correlated the applied load to the frame or time in seconds. An area of the image was then selected for analysis. See figure 15 for a representative image of data selection area. A graph of the intensity versus pixel size was created to locate the center of the mini-implant head and an image was then generated that plotted time (record number) versus pixel position for the reference and sample region. See figure 16. From this information data points were graphed on a displacement (μm) to distance

from mini-implant head (mm) graph and a best fit line was generated. See Figure 17. The derivative of this best fit line was used to generate a straight line to evaluate displacement (μm) for distances 2.0 mm and greater from the mini-implant head. Calculations were made to describe the specific strain (με/N) as related to the distance from the mini-implant center and a graph was generated for each sample.

Statistical Analysis

Data were analyzed with a series of 2 x 3 factorial analysis of variance (ANOVA). The independent variables were cortical bone thickness (1.0 mm, 1.5 mm and 2.0 mm) and mini-implant collar type (with or without collar). The dependent variables were force to mini-implant displacement 0.5 mm, force to mini-implant displacement 1.0 mm, force to mini-implant displacement 1.5 mm, force to yield point, maximum insertion torque (MIT) and slope of the force deflection curve (slope). The means and standard deviations for each dependent variable are presented in Table 2. To ensure the data met ANOVA assumptions, histograms were plotted to check for normality of the data, while Levene's test was conducted to ensure homogeneity of variance. In some instances, the homogeneity assumption was violated. However, ANOVA is robust to violation of homogeneity if the normality and independence assumptions are met.

Tukey's post-hoc testing was done to determine significance levels between mini-implants with collars and those without collars for each independent variable and each cortical bone thickness group. Any significant interaction between independent variables was plotted for further interpret the interaction. This method was preferred to analysis of simple main effects due to the small sample size. If no interaction existed, the main effect was examined for significance. If significant, pair-wise comparisons using the Tukey method were used to determine which pairs of means were significantly different. All null hypotheses were rejected at the $p < 0.05$ level.

ESPI

ESPI provides qualitative and quantitative information. For the purposes of this study qualitative information is presented and quantitative values are reported for all samples (n=8) but further statistical analysis was limited.

RESULTS

Mean anchorage force resistance values to crosshead displacement were collected for each sample at three points (0.5 mm displacement, 1-0 mm displacement, 1.5 mm displacement). In the current study yield point indicates the point at which permanent deformation of the synthetic bone analogue occurs. All dependant variables and the descriptive statistics mean, standard deviation, kurtosis and skewness are shown in Table 2. The cortical bone thickness, presence of collar and dependent variables relating to anchorage force resistance at the three crosshead displacement points are shown with their means and standard deviations in Table 3. As anticipated, the mean anchorage force resistance values increased as the crosshead displacement distance increased in all groups. The ranges of the mean anchorage force resistance values to 0.5 mm crosshead displacement (111.74 N ± 6.09 to 197.62 N ± 33.93) were the smallest while the range at 1.5 mm crosshead displacement (147.06 N ± 14.78 to 347.62 N ± 18.67) were the largest. The mean anchorage force resistance values for crosshead displacement also increased as the thickness of the cortical bone increased in both mini-implant groups. The lowest mean anchorage force resistance values were found in the thinnest cortical bone (1.0 mm), while the highest were found in the thickest cortical bone (2.0 mm). The lowest mean anchorage force resistance value was 111.74 N ± 6.09 . This was the mean anchorage force resistance to crosshead displacement 0.5 mm in thin cortical bone (1.0 mm). The highest mean anchorage force resistance value was 347.62 N ± 18.67. This was the mean anchorage force resistance to crosshead displacement 1.5 mm and was found in thick cortical bone (2.0 mm).

The mean anchorage force resistance values to crosshead displacement 0.5 mm, 1.0 mm and 1.5 mm were greater for mini-implant groups with collars than for mini-implant groups without collars in all cortical bone thicknesses (1.0 mm, 1.5 mm and 2.0 mm). The range of mean anchorage force resistance values to crosshead displacement 0.5 mm for mini-implants with collars (145.70 N ± 25.14 to 197.62 N ± 33.93) was greater than for mini-implants without

collars (111.74 N ± 6.09 to 127.64 N ± 34.00). The range of mean anchorage force resistance values to crosshead displacement 1.0 mm for mini-implants with collars (199.76 N ± 26.20 to 292.66 N ± 31.16) was greater than for mini-implants without collars (144.38 N ± 4.19 to 184.32 N ± 38.45). The range of mean anchorage force resistance values to crosshead displacement 1.5 mm for mini-implants with collars (224.16 N ± 21.83 to 347.62 N ± 18.67) was greater than for mini-implants without collars (147.06 N ± 14.78 to 198.07 N ± 44.29).

Two by three way analysis of variance for the dependent variable mean anchorage force resistance to displacement 0.5 mm showed significant differences between mini-implant groups (P=0.0002), and cortical bone thickness groups (P=0.0026), as well as a significant interaction between variables (mini-implant x cortical bone thickness, P=0.0325; see table 5). Tukeys post-hoc analysis showed there was a significant difference in the 2.0 mm cortical bone thickness groups for mini-implants with a collar when compared to mini-implants without a collar (P=0.0013). There was not a significant difference in either the 1.0 mm cortical bone thickness group (P=0.2505) or 1.5 mm cortical bone thickness group (P=0.9808) for mini-implants with a collar when compared to mini-implants without a collar (Figure 7).

Two by three way analysis of variance for the dependent variable mean anchorage force resistance to crosshead displacement 1.0 mm showed significant differences between mini-implant groups (P<.0001), and cortical bone thickness groups (P<.0001), as well as a significant interaction between variables (mini-implant x cortical bone thickness, P=0.0193; see Table 6). Tukeys post- hoc analysis showed there was a significant difference in the 1.0 mm cortical bone thickness groups for mini-implants with a collar when compared to mini-implants without a collar (P=0.0491). In addition, there was a significant difference in the 2.0 mm cortical bone thickness group for mini-implants with a collar when compared to mini-implants without a collar (P<.0001). There was not a significant difference in the 1.5 mm cortical bone thickness groups

for mini-implants with a collar when compared to mini-implants without a collar (P=0.5274; see Figure 8).

Two by three way analysis of variance for the dependent variable mean anchorage force resistance to crosshead displacement 1.5 mm showed a significant difference between mini-implant groups (P<0.0001), cortical bone thickness groups (P<0.0001), as well as a significant interaction between variables (mini-implant x cortical bone thickness, P=0.0140; see Table 7). Tukeys post-hoc analysis showed there was a significant difference in the 1.0 mm cortical bone thickness group (P=0.0041), 1.5 mm cortical bone thickness group (P=0.0146) and 2.0 mm cortical bone thickness group (P<.0001) when mini-implants with collars were compared to a mini-implants without collars. (see Figure 9).

The means and standard deviations are shown for the dependant variables anchorage force resistance at yield point, MIT and slope based on cortical bone thickness groups and mini-implant groups (Table 4). The mean anchorage force resistance to yield point was greater as the cortical bone thickness increased from 1.0 mm (87.28N ± 26.53) to 2.0 mm (187.42 N ± 27.89). The mean anchorage force resistance to yield point was greater for mini-implant groups with collars (105.52 N ±15.83 to 187.42 N ± 27.89) compared to mini-implant groups without collars (87.28 N ± 26.52 to 93.88 N ± 49.36) in each cortical bone thickness tested (1.0 mm, 1.5 mm and 2.0 mm).

Two by three way analysis of variance for the dependent variable mean anchorage force resistance to yield point showed significant differences between mini-implant groups (P=0.0004), and cortical bone thickness groups (P=0.0063), as well as a significant interaction between variables (mini-implant x cortical bone thickness, P=0.0145; see Table 8). Tukeys post-hoc analysis showed there was a significant difference in the 2.0 mm cortical bone thickness groups for mini-implants with a collar when compared to mini-implants without collars (P=0.0005). There was not a statistically significant difference in the 1.0 mm cortical bone thickness groups for mini-implants with a collar when compared to mini-implants without collars

(P=0.9216). In addition, there was not a statistically significant difference in the 1.5 mm cortical bone thickness groups for mini-implants with a collar when compared to mini-implants without collars (P=0.8202; see Figure 8).

The mean MIT values increased as the cortical bone thickness increased. The range of MIT values in 1.0 mm cortical bone (18.84 Ncm ± 1.99 to 21.4 Ncm ± 1.79) were less than the values recorded in 2.0-mm cortical bone (24.18 Ncm ± 3.57 to 29.36 Ncm ± 5.21). The mean MIT values for mini-implants with collars were higher than the mean MIT values for mini-implants without collars in two cortical bone thickness groups (1.0 mm and 2.0 mm) but the opposite was true for the 1.5 mm cortical bone thickness group.

Two by three way analysis of variance for the dependent variable MIT showed a significant difference between cortical bone thickness groups (P=0.0002) but not mini-implant groups (P= 0.0659). There was no significant interaction between the variables (mini-implant x cortical bone thickness, P = 0.1075; see Table 9). Pairwise comparisons of the means showed the MIT of the 1.0-mm cortical bone thickness group was significantly less than both the 1.5 mm cortical bone thickness group (P=0.0019) and the 2.0-mm cortical bone thickness group (P=0.0003). The 1.5 mm cortical bone thickness group was not significantly different than the 2.0 mm cortical bone thickness group (P=0.8130; see Figure 9).

The mean values for the slope of the mean anchorage force deflection curves increased as the cortical bone thickness increased. The range for the mean slope values in the 1.0 mm cortical bone thickness group (251.26 ± 39.88 to 354.98 ± 74.61) were less than the range for the mean slope values in the 2.0 mm cortical bone thickness group (264.54 ± 62.28 to 389.30 ± 68.38). The range in mean slope values for mini-implant groups with collars (354.98 ± 74.61 to 389.30 ± 68.38) were greater than those for mini-implant groups without collars (251.26 ± 39.88 to 264.54 ± 67.28) at all cortical bone thicknesses.

Two by three way analysis of variance for the dependent variable slope of the mean anchorage force resistance to displacement curve was significantly different between mini-implant groups (P=0.0013) but not cortical bone thickness groups (P= 0.2187; see Table 10). In addition, there was no significant interaction between variables (mini-implant x cortical bone thickness, P=0.0930). Pair-wise comparisons of the means showed that the slope of the mean anchorage force resistance to displacement curve was significantly greater for mini-implant groups with collars compared to the mean anchorage force resistance to displacement curves of mini-implants without collars (P=.0013; see Figure 10).

ESPI

Figure 16 shows the typical real time speckle pattern showing in-plane displacement in the x-direction on the bone analogue surface adjacent to the mini-implant recorded by the CCD camera and displayed on the computer monitor. It was observed that the region of bone analogue closest to the mini-implant was the first region to exhibit a correlation pattern. As the applied load increased, the number of speckle fringes in the region increased. Further, at higher load levels fringes appeared at regions more distant from the mini-implant. It was observed that fringes radiated from the mini-implant in a circular pattern. The number of fringes sequentially increased as the magnitude of the applied load increased from 0 to 30 N.

Table 11 shows the quantitative strain values collected. The specific strain values ($\mu\varepsilon$/N) at 2.0 mm from the mini-implant head range from 3.24 $\mu\varepsilon$/N to 37.50 $\mu\varepsilon$/N. For mini-implants loaded multiple times the specific strain values at 2.0 mm were greater (12.45 $\mu\varepsilon$/N to 37.5 $\mu\varepsilon$/N) compared with mini-implants loaded initially (3.24$\mu\varepsilon$/N to 8.0$\mu\varepsilon$/N). In addition a trend existed that mini-implants with collars had less strain 2.0 mm from the mini-implant head.

The specific strain zero point (mm) reveals the distance from the mini-implant head where specific strain (με/N) reaches zero. The range of values collected was from 2.85 mm to 4.67 mm.

The slope of the specific strain (με/N) displacement curve was greater for the mini-implant group loaded multiple times (12.66-30.00) compared with mini-implants loaded initially (3.81- 8.42). In addition, a trend existed that mini-implants with collars had smaller slope values.

The mini-implant head displacement values were greater for mini-implants loaded multiple times (1.02μm/N to 2.07μm/N) than for mini-implants loaded initially (.66μm/N to 1.57μm/N). In addition, mini-implants with collars had less mini-implant head displacement in both load groups.

DISCUSSION

The metal jig prematurely dislodged from the mini-implant before it was displaced 1.5 mm for two samples in the 2.0 mm cortical bone thickness group, one with a collar and one without a collar. In both cases, this occurred after the yield point had been reached. Therefore, the dependent variable mean anchorage to force displacement 1.5 mm in the 2.0 mm cortical bone thickness group had a reduced sample size of eight (N=8; see Table 3).

The mean anchorage force resistance values collected were based on those of Brettin *et al.* (2009) who stated that 1.5 mm mini-implant displacement was the point at which clinical failure was eminent (Brettin *et al.*, 2008). Figures 7, 8, 9 and 10 show that in all three cortical bone thickness groups (1.0 mm, 1.5 mm and 2.0 mm) the mean anchorage force resistance values at crosshead displacement 0.5 mm, 1.0 mm and 1.5 mm had already exceeded the yield point. Therefore, all mean anchorage force resistance values collected are in the plastic range of the bone analogue material. In addition, the yield point in all three cortical bone thickness groups tested (1.0 mm, 1.5 mm and 2.0 mm) was greater than the typical clinical load applied to an orthodontic mini-implant. Forces placed on mini-implants can vary widely and typical orthodontic loads are approximately 0.3 to 4 N, or roughly 30 to 400 grams, depending on the desired tooth movement (Ren et al., 2003). The more important finding may be to determine the differences between mini-implant groups in the elastic region, prior to reaching the yield point, as this is the range where clinically applicable loads are applied. Mini-implant loss rates are variable and high yet the forces applied are lower than the yield points described in the present study. Clearly, the biological responses of living tissue play a role in mini-implant failures and a purely mechanical study will not adequately reveal this.

Overall, mini-implants with collars provided increased anchorage force resistance compared with mini-implants without collars. As illustrated in Figures 7, 8, 9 and 10 the mean

anchorage force resistance values for mini-implants with collars exceeded those of mini-implants without collars in all three cortical bone thicknesses tested (1.0 mm, 1.5 mm and 2.0 mm). This was true for mini-implant mean anchorage force values collected at the mini-implant deflection points 0.5 mm (P=0.0002), 1.0 mm (P<.0001) and 1.5 mm (P<0.0001). The mean anchorage force resistance values were also significantly greater as the cortical bone thickness increased, regardless of the presence of a collar. This was true for mini-implant mean anchorage force values collected at the mini-implant deflection points 0.5 mm (P=0.0026), 1.0 mm (P<.0001) and 1.5 mm (P<.0001). This finding agrees with Brettin *et al.* (2008), who found that mandibular bone sites, with greater cortical bone thickness, offered significantly greater mean force resistance than did maxillary bone sites for both 1.5 mm and 2.5 mm monocortical mini-implants. The present study differs from Brettin *et al.* (2008) in that the current studies mean anchorage force resistance values are higher but similar. This is not surprising given the present study used a synthetic bone analogue and the Brettin *et al.*(2008) study used cadaver bone. Human cadaver bone replicates the microstructure structure of vital bone to a higher degree than a synthetic bone analogue could, yet still has limitations compared to a living tissue. The values are similar because both are non-vital structures that do not take into account the biological responses occurring in living tissues.

In the present study, there was a significant interaction between the independent variables cortical bone thickness and mini-implant type at the mini-implant deflection points 0.5 mm, 1.0 mm and 1.5 mm. As illustrated and interpreted in Figures 7, 8 and 9 the presence of a collar had a greater affect on the mean anchorage force resistance when the cortical bone thickness was greater. The highest mean anchorage force resistance was found for mini-implants with collars in 2.0 mm cortical bone. Mechanically, this is logical as the force distribution to bone is different in mini-implants with collars when compared to mini-implants without collars. Mini-implants with collars engage the cortical bone with the base of the collar as well as the mini-implant body when a horizontal force is applied. Mini-implants without collars engage bone

only with the mini-implant body itself. Mini-implants with collars, therefore, engage a greater volume of cortical bone. Furthermore, this volume of cortical bone becomes even greater as the thickness of cortical bone increases from 1.0 mm to 2.0 mm. The thickness of cortical bone is significant in that the higher modulus material, or stiffest material, is the material that will offload most of the force. This finding suggests clinically that the advantage of placing a mini-implant with a collar is greatest in areas with cortical bone thicknesses near 2.0 mm such as the mandible (Parke et al., 2002), infrazygomatic crest (Liou et al., 2004) and palate (Deguchi et al., 2006). However, at all cortical bone thicknesses the collar increased mean anchorage force resistance likely due to offloading to the cortical bone.

Mini-implants with collars had significantly higher yield points when compared with mini-implants without collars (P=0.0004). Therefore, more force was required for mini-implants with collars to permanently deform the bone analogue when compared to those mini-implants without collars. As illustrated in Figure 10, the mean anchorage force resistance values for the yield points of mini-implants with collars exceeded those of mini-implants without collars in all three cortical bone thicknesses tested (1.0 mm, 1.5 mm and 2.0 mm). In addition, the mean anchorage force resistance values for the yield points of mini-implants with collars was significantly greater as the cortical bone thickness increased (P=0.0063). There was also a significant interaction between the independent variables cortical bone thickness and collar. Post-hoc testing revealed the mean anchorage force resistance value for the yield point was significantly greater for mini-implants with collars in the 2.0 mm cortical bone thickness group when compared to mini-implants without collars (p=0.0005). The presence of a collar appeared to have a greater affect on the mean anchorage force resistance value for yield point when the cortical bone thickness was greater. The explanation for this again is based upon the greater volume of the higher modulus cortical bone.

The slopes of the mean anchorage force displacement curves were significantly different when comparing collar groups (p=0.0013) but not cortical bone thickness groups (P=0.2187).

That the slopes are different suggests that with an applied force the amount of mini-implant displacement for a mini-implant with a collar will be less than that of a mini-implant without a collar. This also suggests less bone strain may occur for mini-implants with a collar when compared to those without a collar. This finding agrees with Morarend et al. (2009) who found that a 2.5 mm monocortical mini-implant, with a larger surface area, provides superior anchorage resistance compared with a 1.5 mm mono-cortical mini-implant, with a smaller surface area (Morarend et al., 2009). This finding contrasts with the findings of Miyawaki et al. (2003) who reported no difference in the 1-year success rates of 2.3 and 1.5 mm mini-implants (85% and 84% success, respectively). However, they reported a success rate of 0.0% for the 1.0 mm diameter mini-implants (Miyawaki et al., 2003). Therefore, diameter and surface area do appear to play a role clinically, but the effect may be less pronounced at lower loading with larger-diameter and greater surface area mini-implants.

The cortical bone thickness had a significant affect on MIT (P=0.0002), while the presence of a collar did not (P=0.0659). As illustrated in Figure 11 the MIT was significantly greater for 1.5 mm when compared with 1.0 mm cortical bone thickness (P=0.0019) and significantly greater for the 2.0 mm cortical bone thickness when compared to the 1.0 mm cotical bone thickness (P=0.0003) but there was no difference between the 1.5 mm and 2.0 mm cortical bone thickness groups. Care was taken to use a bone analogue with physical properties similar to human bone. The mean MIT for mini-implants in human subjects was reported to range from 7.2 to 13.5 Ncm (Motoyoshi et al., 2006). These were lower MIT values than collected in the present study. However, Song et al. (2007), using a bone analogue with similar physical properties also reported higher MIT values (Song et al., 2007). MIT values in the present study were used as a method to eliminate or reveal error created by over-tightening orthodontic mini-implants with collars.

The ESPI portion of the present study was significant in that it quantified microstrain ($\mu\varepsilon$) values found in the surrounding bone analogue when clinically relevant forces were applied.

Interestingly, specific microstrain values ranged from 12.45 με/N – 37.50 με/N at a distance of 2.0 mm from the mini-implant-bone analogue interface. Comparing these values to those determined by Frost et al. we see that these values lie below the upper limit of bone equilibrium, 1,000 με to 1,500 με. Bone formation is the initial response about this limit. Additional strain, however, leads to microfissure and microfracture and at 3,000 με it is thought that the ongoing repair process of bone is surpassed and bone resorption occurs (Frost, 2004). Most bone is under constant strain so it is feasible that adding additional strain to an existing and unknown strain value in some instances will lead to bone resorption.

It appears that specific strain values and slope values are greater when mini-implants are loaded multiple times when compared to one initial loading. This may be due to plastic deformation in the cancellous portion of the bone analogue. Clinically, this suggests single loadings with continuous force, as in indirect anchorage, may be decrease strain values in the surrounding bone.

A trend exists that mini-implants with collars produces less strain in the surrounding cortical bone. Given the present ESPI configuration we were not able to evaluate the strain levels directly at the implant-bone interface to 2.0 mm from the mini-implant center. However, there appears to be 40% less mini-implant head displacement for mini-implants with collars when compared to mini-implants without collars. This was true while loading the mini-implants initially as well as multiple times. Clearly this phenomenon is beneficial and further studies will be needed to determine the clinical relevance.

Recently, Huja et al. (2005), reported pull-out strengths of monocortical mini-implants placed in the maxillae and mandible of dogs from 134 N to 388 N (Huja et al., 2005). These forces are somewhat greater than, but similar to, the force levels we reported here. Although these force levels are greater than those normally used to move teeth, well-controlled in-vitro studies such as these provide valuable insights into anchorage. Furthermore, greater forces are often used by orthodontists to treat patients orthopedically. For instance, after placement of

mini-plates on the lateral nasal wall for anchorage, Kircelli et al. (2005), applied facemask protraction to an 11-year-old girl with severe maxillary hypoplasia. The forces applied to the plates were 150 to 350 g (Kircelli et al.,2005). These forces remain less than the yield points for all groups in the present study. The mini-implant collar clearly shows the potential to impact strain distribution to the surrounding bone tissue, yet further studies are needed to support this in-vitro study.

Clinically, the advantage of a larger mini-implant is its ability to distribute applied forces over greater areas of bone with less bone stress. The drawback of a larger mini-implant is the surrounding anatomic limitations. Morarend et al. (2009) suggested one alternative is a narrower bicortical mini-implant (Morarend et al., 2009). The results of this study indicate that another alternative is a mini-implant with a collar. A mini-implant with a collar, like a bicortical mini-implant, is advantageous when there is insufficient room interproximally to place a large diameter mini-implant.

The biologic changes on osseous loading could not be examined in this in-vitro study. However, unlike traditional endosseous implants, which need a waiting period for bone healing and osseointegration, the primary stability of mini-implants is believed to result from mechanical retention of the mini-implant in the bone (Costa et al.,1998; Liou et al., 2004). In-vitro studies of mini-implants should, therefore, more closely replicate the immediate loading response in situ immediately after placement.

The finding that a mini-implant collar placed in direct contact with cortical bone decreases bone strain on the compression side also suggests that placement protocols should address gingival tissue to ensure mini-implant collars are in contact with cortical bone. This may lead to future recommendations to penetrate the gingival tissue prior to implant placement or to have threads on the mini-implant collar to encourage cortical bone contact.

LIMITATIONS:

It is unlikely that all mini-implants are placed perpendicular to the cortical bone surface with the collar in direct contact with cortical bone. Clinically, this is not always possible due to variability in the bony architecture of the maxilla and mandible as well as the thickness of gingival tissue. The mini-implant used in this study is manufactured and recommended for use in the anterior region of the maxilla and mandible, where gingival thickness typically is less than that in the posterior maxilla or mandible. However, different periodontal biotypes (phenotypes) do exist, with great interindividual and intraindividual variations (Mueller & Eger 2002; Goaslind et al., 1977). In order to achieve contact, in all cases the gingival tissue would need to be removed either by a tissue punch, a bur, or threads on the mini-implant collar.

Our study used a synthetic bone analogue with similar mechanical properties to human cortical and cancellous bone. This in-vitro study could not take into account the responses of a living biological tissue. However, using a bone analogue allowed us to control the cortical bone thickness and mechanical properties to make valid comparisons in an in-vitro mechanical study.

ESPI in-plane is evaluating surface strain only in the x-axis. The collar and mini-implant head inhibit the collection of data in the bone analogue directly apical to this. This could be explored with ESPI by evaluating both the x and the y plane.

FUTURE STUDIES:

The current study was a well-controlled in-vitro mechanical study. The current study should be reproduced initially in both human maxillary and mandibular cadaver bone and next in fresh hydrated porcine bone. An animal model utilizing histology to compare the bone response at the implant bone interface for mini-implants with and without collars would be revealing. Variable time periods and force levels would help determine if the mini-implant collar could have an affect on mini-implant stability at clinically applicable load levels.

A randomize prospective clinical study with a sample size of at least 50 mini-implants would be ideal. To attempt to control the variable cortical bone thickness a cone beam CT could be taken prior to mini-implant placement. Mini-implants should be placed on opposite sides in patients needing two mini-implants and in similar locations. For example, mini-implants could be placed in the maxilla, between the second premolar and first molar in the buccal alveolus 6.0 mm from crestal alveolar bone. It would be important to control the timing and magnitude of the load as well as the insertion torque used to place the mini-implant. Overall clinical success could be studied as well as mini-implant displacement by either direct measurement or radiographic measurement. Future studies should help determine if the mini-implant collar minimizes bone strain at clinically relevant load levels to the degree that it affects mini-implant stability and ultimately mini-implant survival.

ESPI is a relatively new optical technique that should be further utilized in dental and more specifically orthodontic research. A lower modulus, less stiff, testing medium such as a photoelastic material may be better suited for the ESPI technique. A mandibular model made of a material with a lower modulus material would allow for strain comparisons to made more easily because fringes would be more numerous and visible at lower force levels. Once this

model was perfected it would be an excellent way to rapidly test many mini-implant characteristics in more than one plane of space or axis. Other orthodontic applications would be to test the claim that different "brackets" produce different strain levels or strain patterns when compared with other brackets under similar conditions. The application of the ESPI technique to orthodontic research could easily be explored on many levels.

CONCLUSIONS

- The mean anchorage force values at crosshead displacements of 0.5-mm, 1.0-mm and 1.5-mm for mini-implants with collars was significantly greater than the mean anchorage force values needed to displace mini-implants without collars.
- The yield point mean anchorage force value for mini-implants with collars was significantly greater than the yield point mean anchorage force value of mini-implants without collars.
- The slope of the loading pattern during deformation was significantly greater for mini-implants with collars than for mini-implants without collars.
- Mini-implant maximum insertion torque (MIT) is independent of the presence of a collar, within the limits of this study.
- The specific strain, slope of the strain displacement curve and mini-implant displacement are greater for mini-implants loaded multiple times than for mini-implants loaded once.
- The mini-implant displacement is less for mini-implants with collars when compared to mini-implants without collars.
- It appears that specific strain 2.0 mm from the mini-implant head is less for mini-implants with collars.

ACKNOWLEDGEMENTS

Thank you to my thesis mentor, Dr. John Mitchell, for guiding and advising me throughout the project.

Thank you to Steve George for his numerous contributions to the project. Your persistence, and enthusiasm were invaluable.

Thank you to Dr. Duncan for guiding us all through the ESPI portion of this study.

Thank you to my thesis committee members, Dr. David Covell and Dr. Larry Doyle, for suggestions and reviewing drafts.

Thank you to Dr. Michael Leo and Dr. Mansen Wang for your statistical support.

Thank you to Dr. Jack Fisher, Ortho TAADS Inc., for donating products to this study.

Thank you to my entire family for their support and understanding.

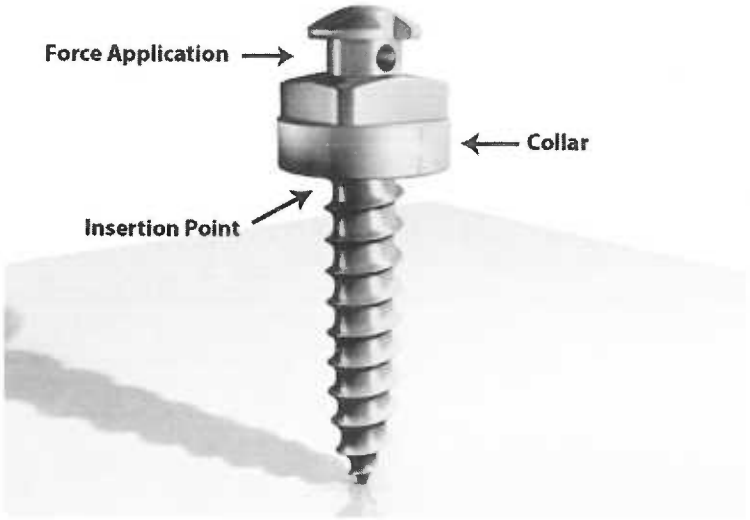

Figure 1. Orthodontic mini-implant with collar: Total mini-implant length (10.5 mm); total threaded length (7.0 mm); insertion point (7.0 mm from tip); collar height (1.0 mm); collar diameter (3.5 mm); force application point (2.5 mm from insertion point or 1.0 mm from head).

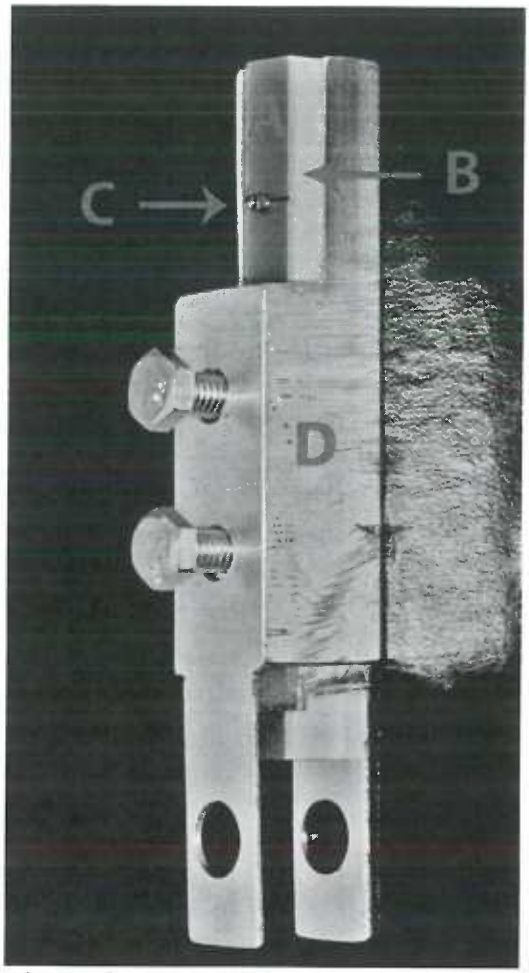

Figure 2. Bone analogue and mini-implant secured in carrier. (A) cortical bone analogue (B) cancellous bone analogue (C) mini-implant (D) custom metal carrier.

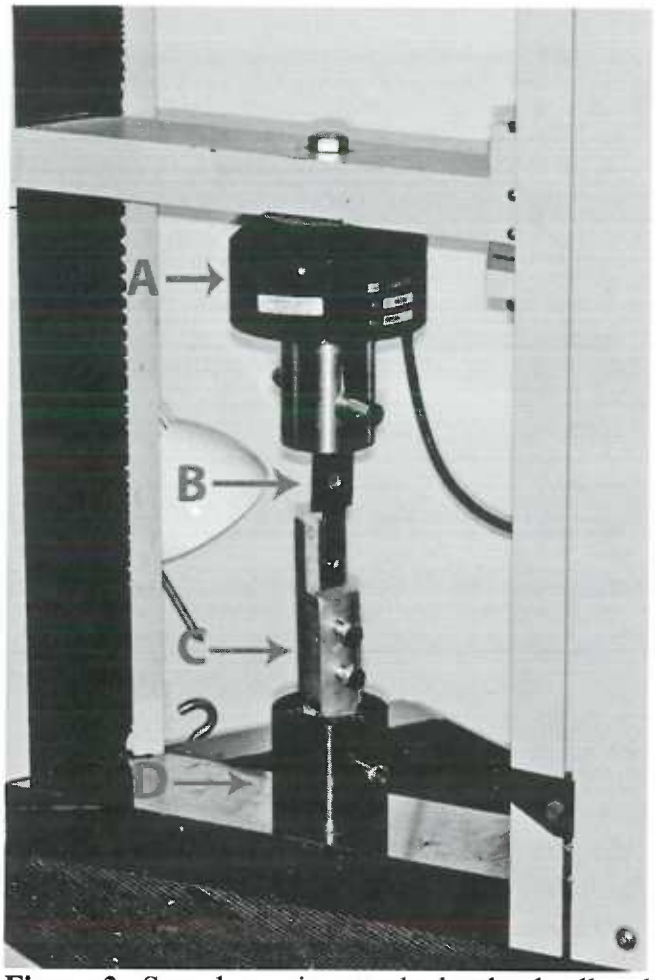

Figure 3. Sample carrier attached to load cell and Q-test machine base (A) load cell (B) jig attached to load cell and mini-implant (C) custom carrier supporting sample (D) machine base.

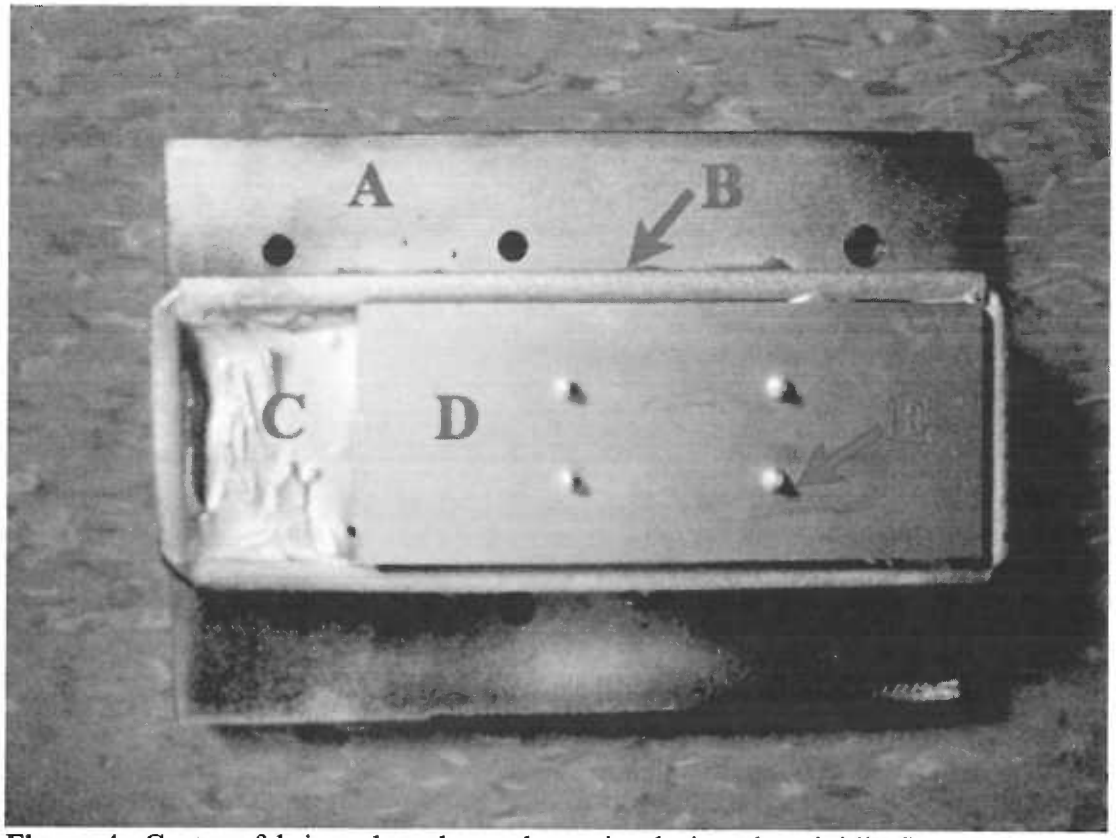

Figure 4. Custom fabricated steel sample carrier designed to rigidly fix sample to optics table. (A) carrier base (B) carrier well (C) lab stone (D) bone analogue (E) mini-implants

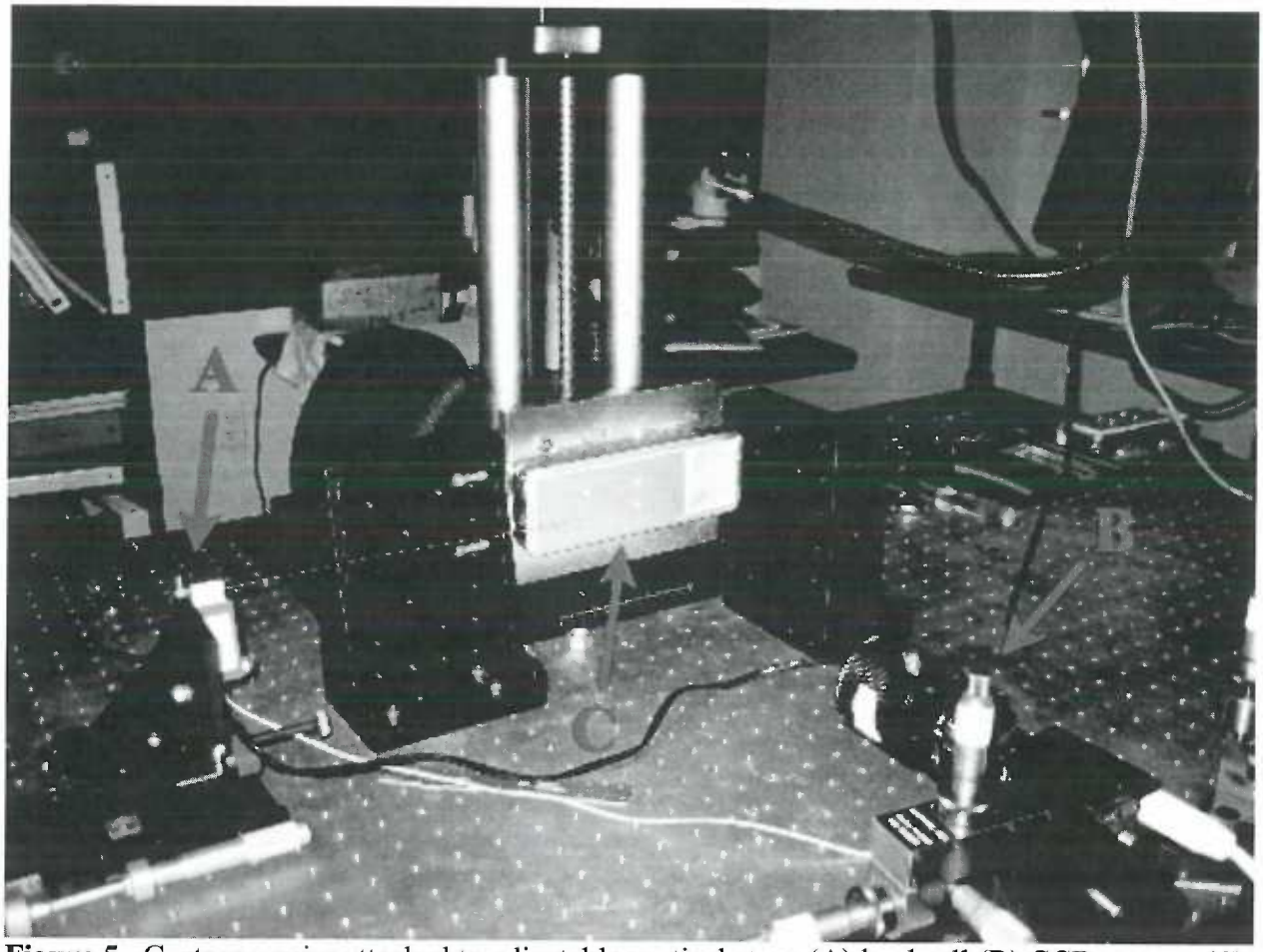

Figure 5. Custom carrier attached to adjustable vertical stage (A) load cell (B) CCD camera (C) sample

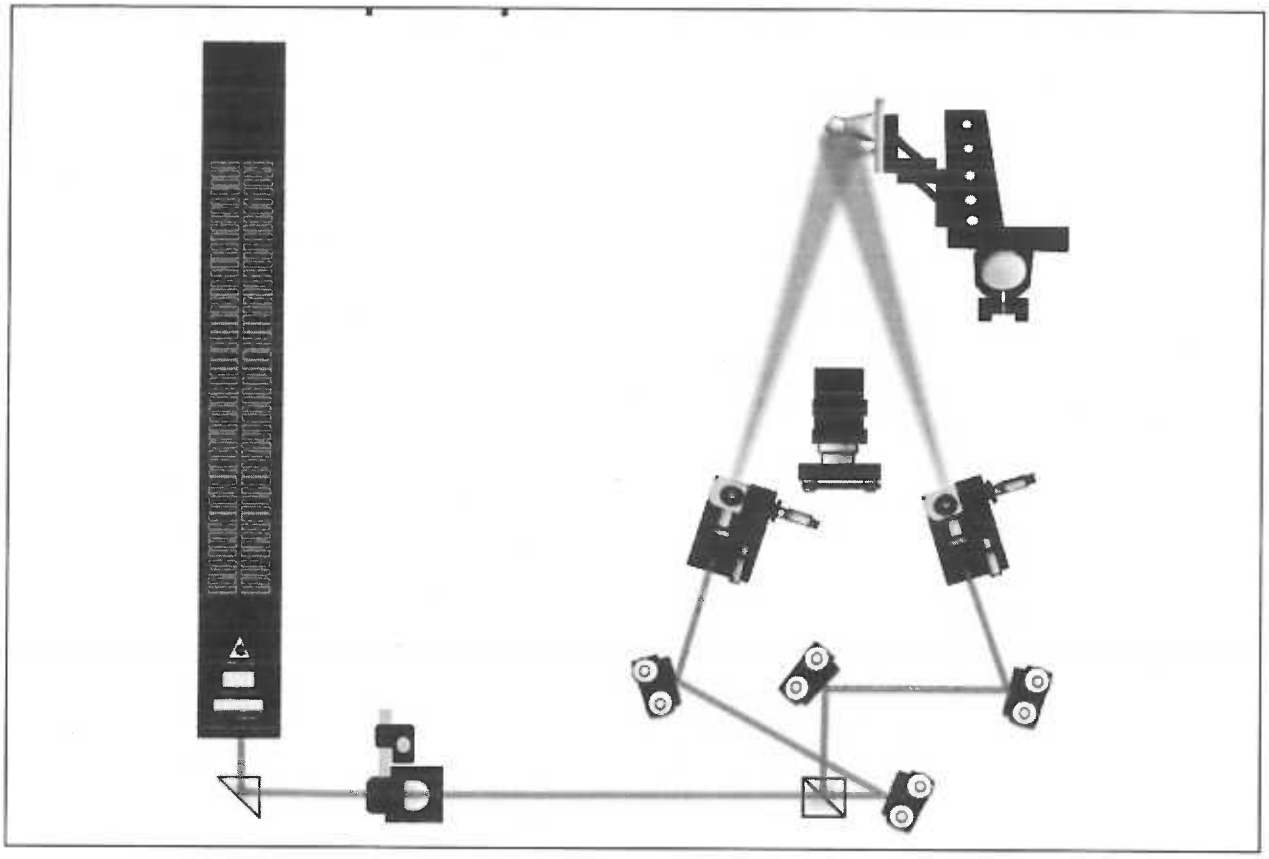

Figure 6. Schematic diagram of in-plane displacement sensitive electronic speckle pattern interferometer.

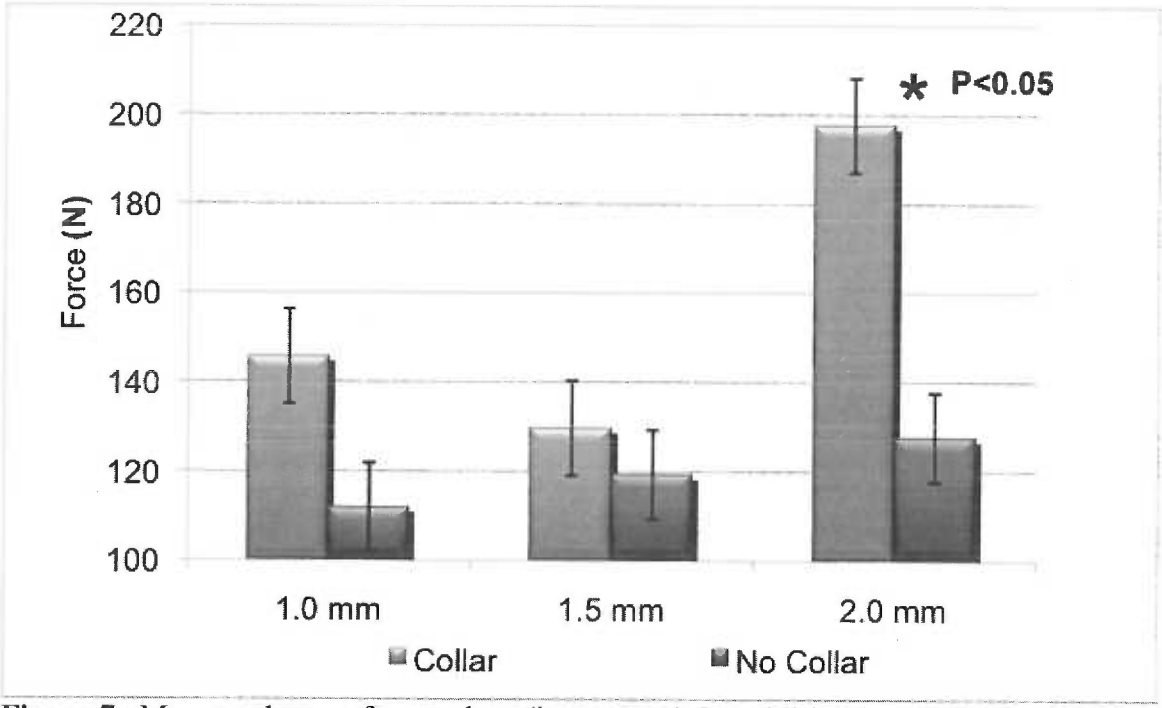

Figure 7. Mean anchorage force values (in newtons) for mini-implant deflection of 0.5 mm vs cortical bone thickness 1.0 mm, 1.5 mm and 2.0 mm for mini-implants with collars and without collars.

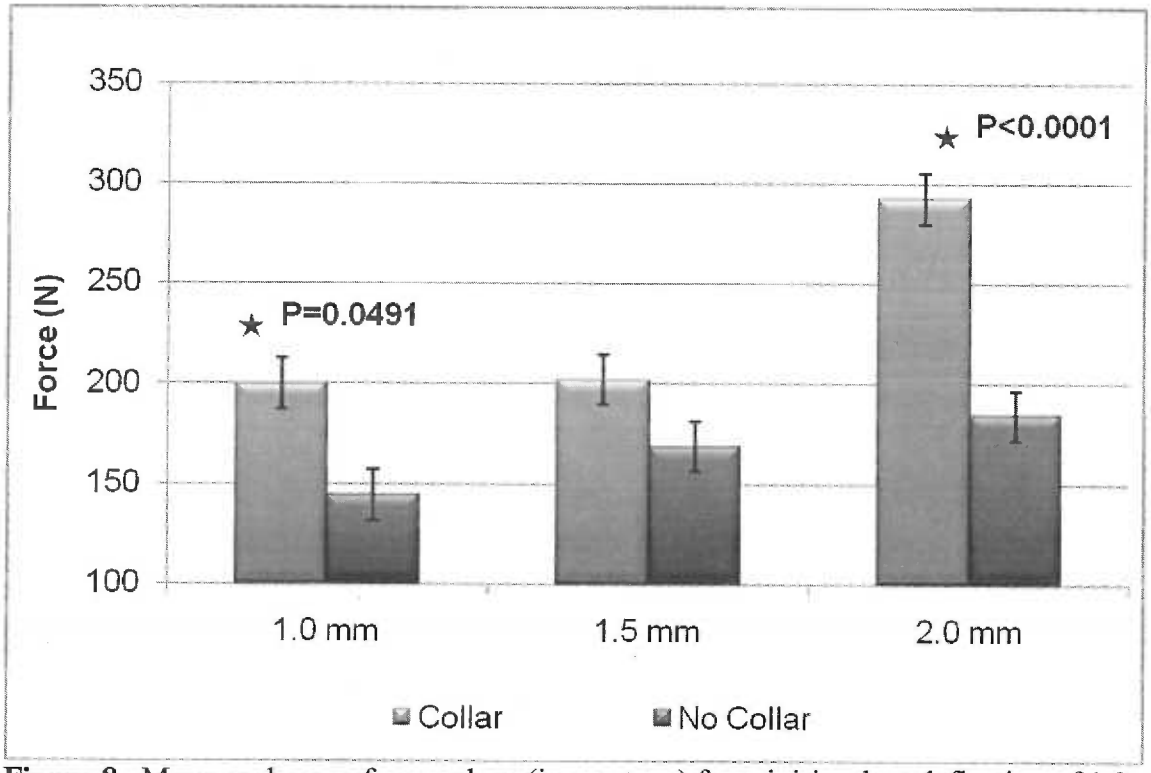

Figure 8. Mean anchorage force values (in newtons) for mini-implant deflection of 1.0 mm vs cortical bone thickness 1.0 mm, 1.5 mm and 2.0 mm for mini-implants with and without collars.

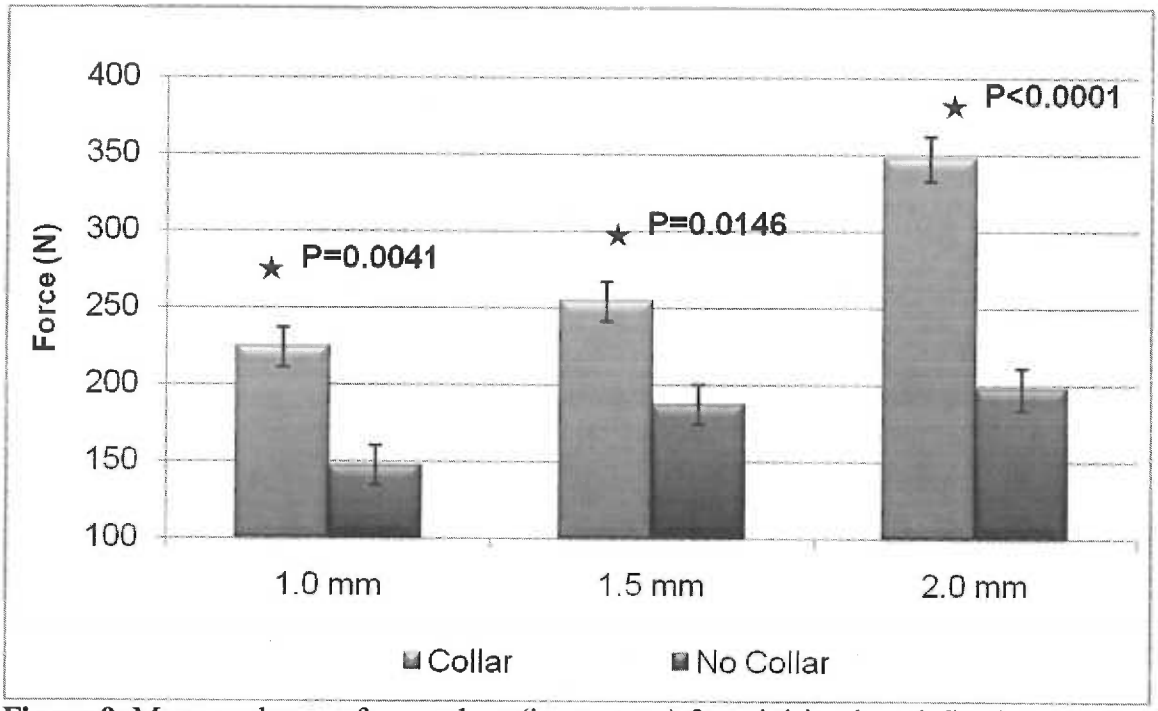

Figure 9. Mean anchorage force values (in newtons) for mini-implant deflection of 1.5 mm vs cortical bone thickness 1.0 mm, 1.5 mm and 2.0 mm for mini-implants with and without collars.

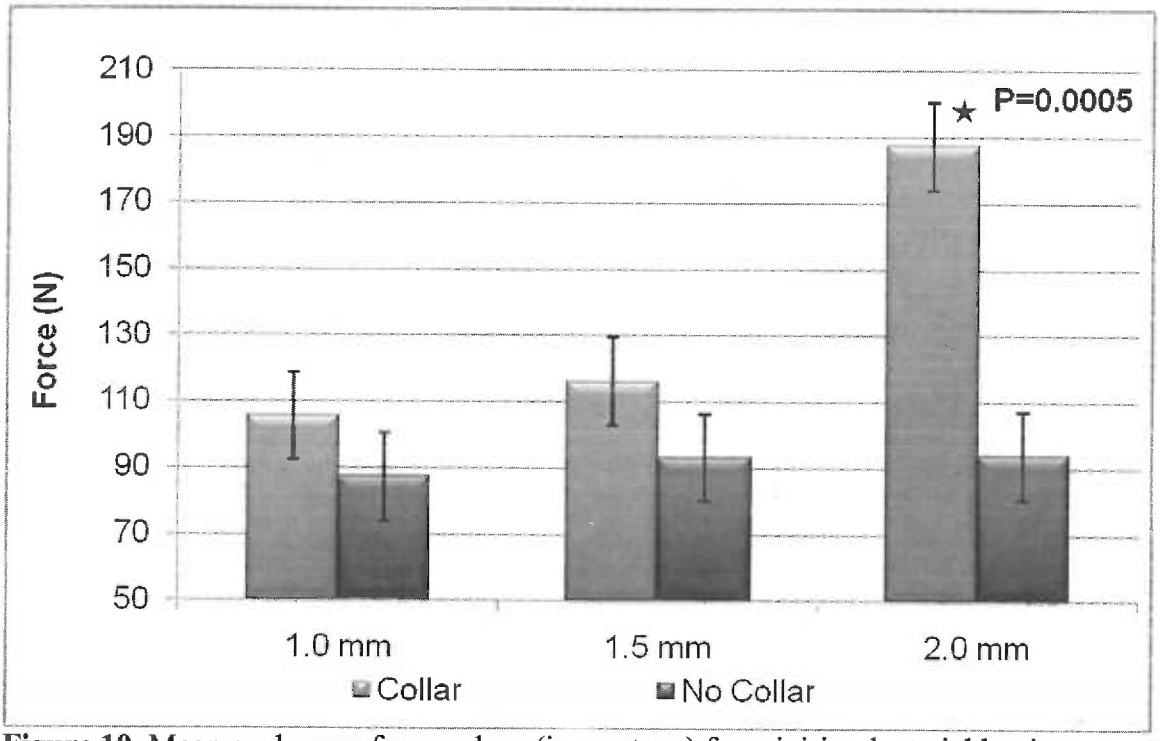

Figure 10. Mean anchorage force values (in newtons) for mini-implant yield point vs cortical bone thickness 1.0 mm, 1.5 mm and 2.0 mm for mini-implants with and without collars.

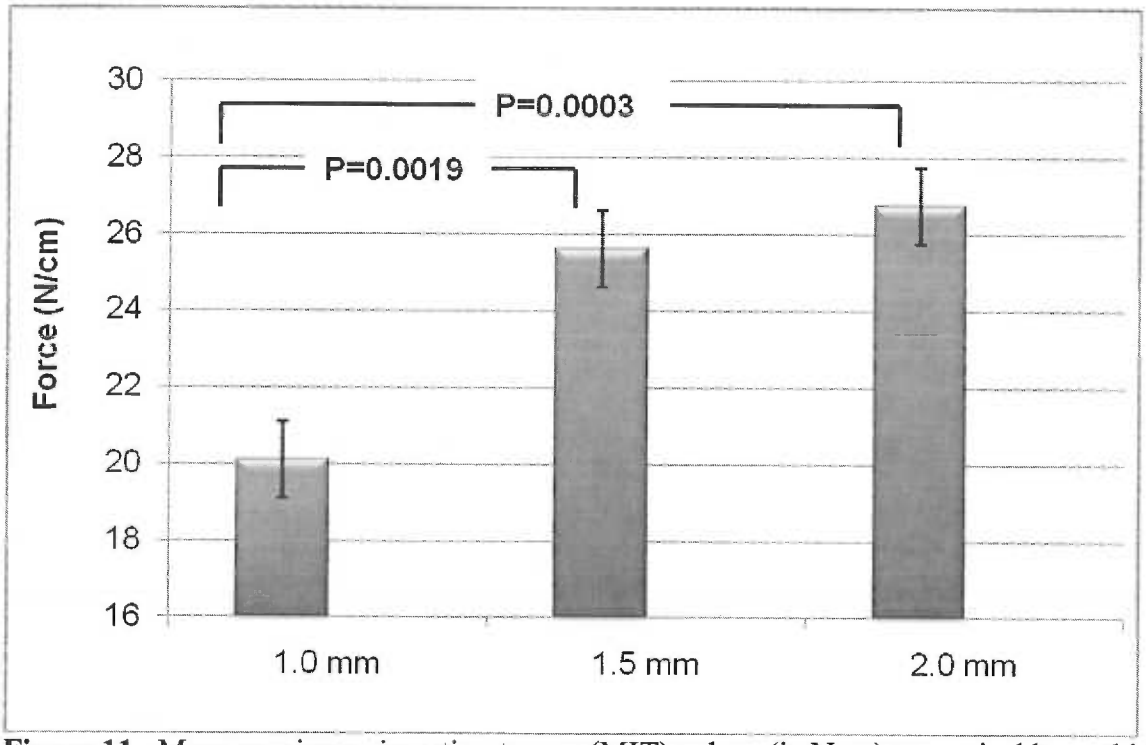

Figure 11. Mean maximum insertion torque (MIT) values (in Ncm) vs cortical bone thickness 1.0 mm, 1.5 mm and 2.0 mm for all mini-implants (n=30).

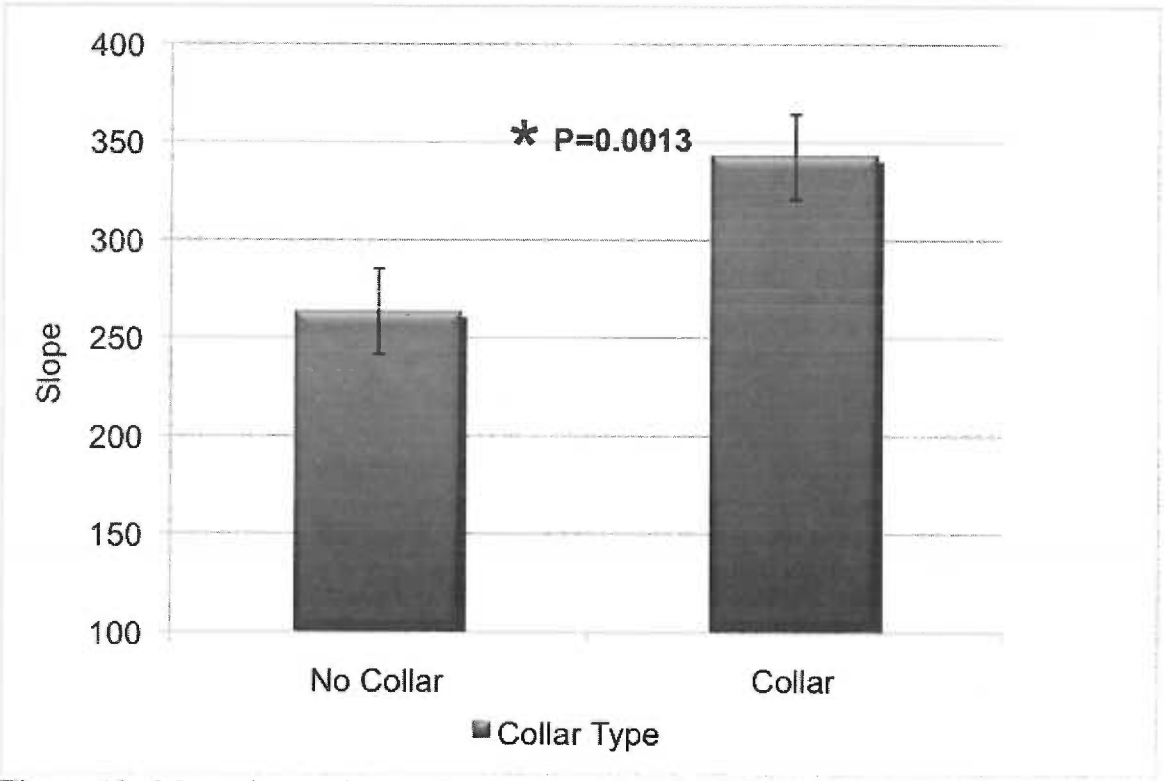

Figure 12. Mean slope values vs implant type for all mini-implants (n=30).

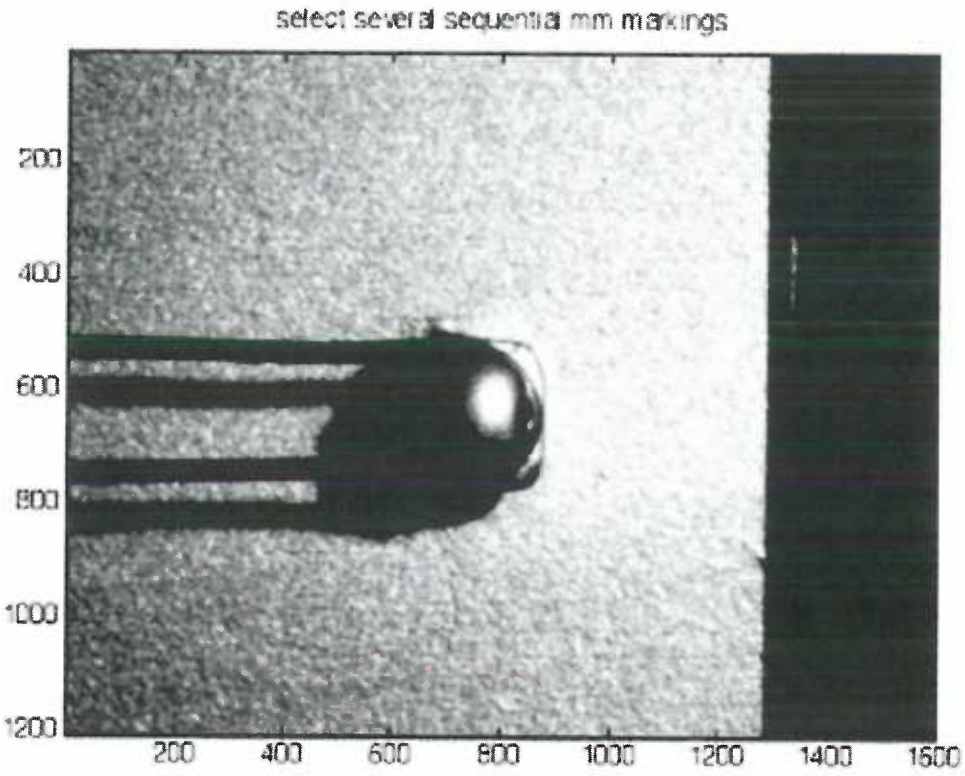

Figure 13. Image of mini-implant with collar and millimeter ruler to relate pixel size to deformation.

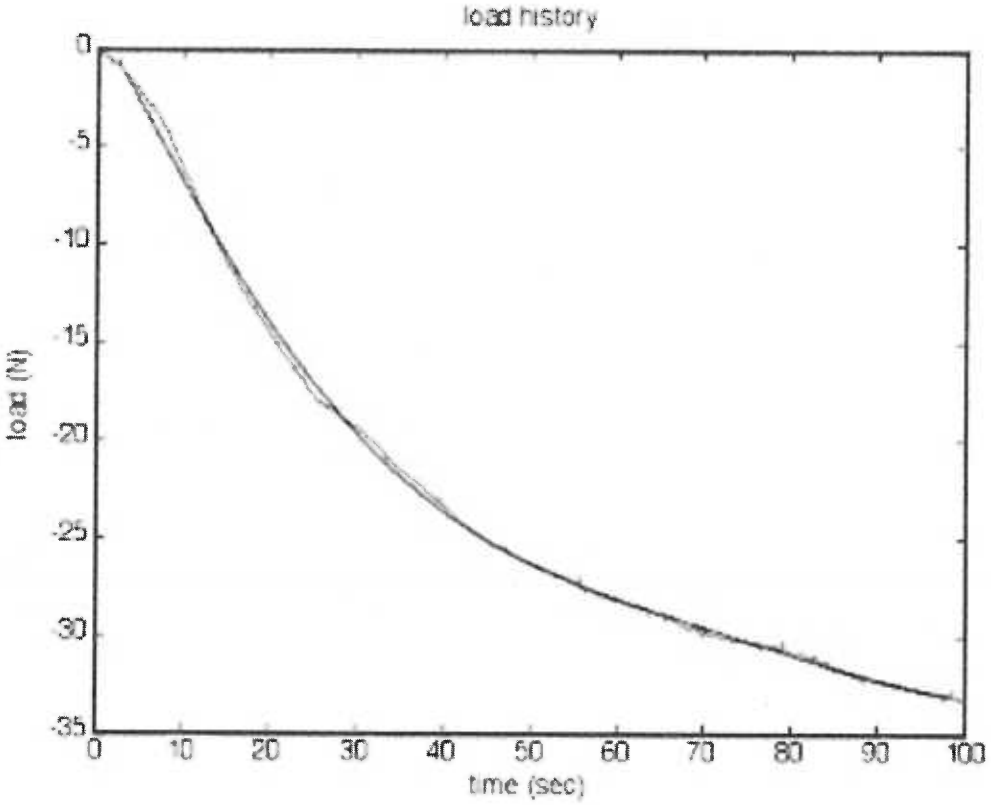

Figure 14. Load history for mini-implant with collar in 2.0 mm cortical bone.

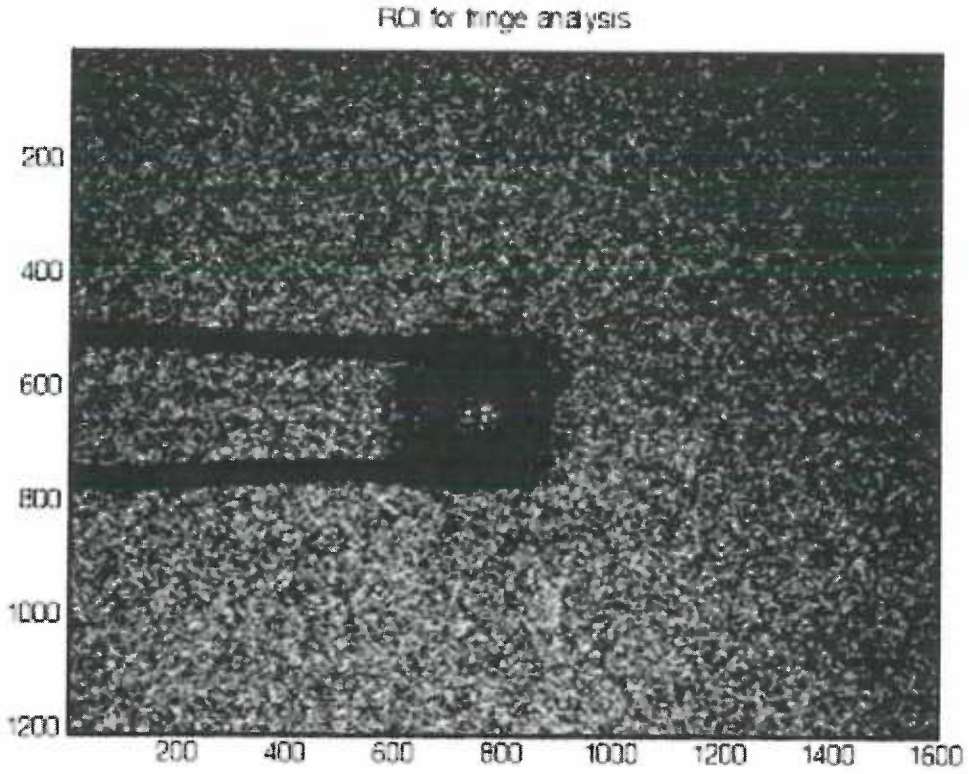

Figure 15. Image showing location of pixels selected to be examined in this study.

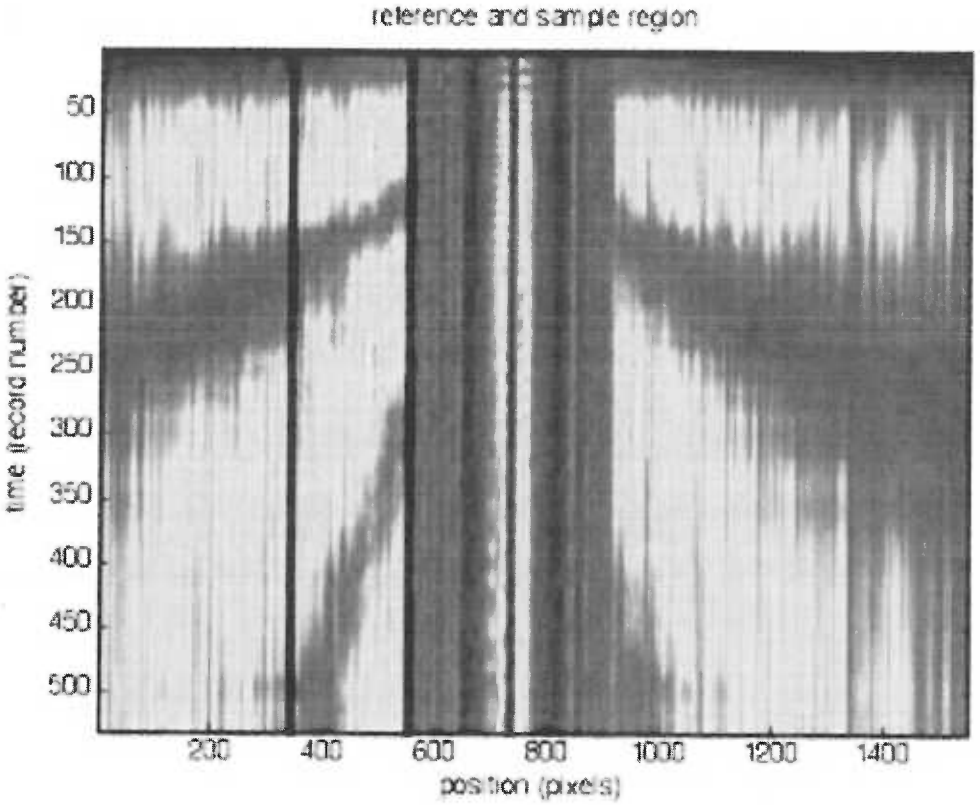

Figure 16. Reference and sample regions. Red line depicts mini-implant head.

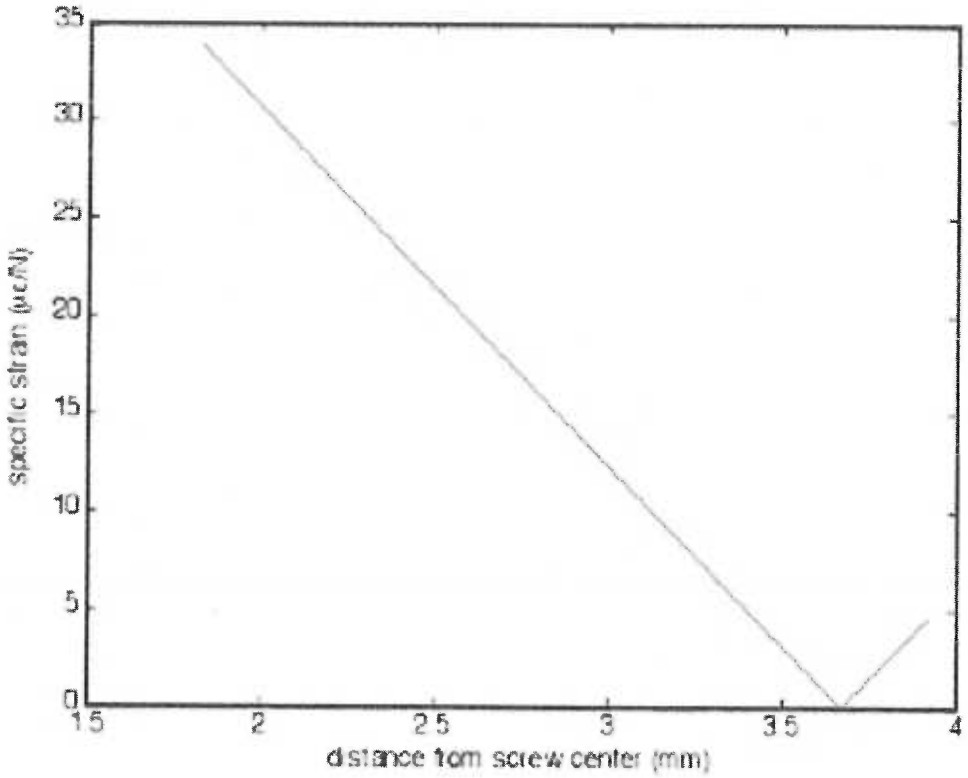

Figure 17. Specific strain vs distance from mini-implant center.

Table 1. Physical properties of bone analogue.

Bone Analogue	Density (g/cc)	Compresive Strength (MPa)	Compressive Modulus (MPa)	Tensile Strength (Mpa)	Tensile Modulus (Mpa)
Cortical Bone	1.64	157	16700	106	16000
Cancellous Bone	0.24	4.9	123	3.7	173

Source: SAWBONES, Pacific Research Laboratories Inc, Vashon Island, WA, USA

Table 2. Dependent variable table showing descriptive statistics.

Dependent Variable	Mean	Std. Deviation	Kurtosis	Skewness	n
Force at crosshead 0.5 mm	138.600	36.0804	1.264	1.210	30
Force at crosshead 1.0 mm	198.667	53.6867	-0.035	0.912	30
Force at crosshead 1.5 mm	223.157	67.5215	-0.355	0.729	28
Yield Point Force	113.913	43.9866	0.463	0.644	30
Maximum Insertion Torque	24.173	4.4705	-0.039	0.478	30
Slope	302.911	75.1512	0.263	0.675	30

Table 3. Data table for dependent variables force to crosshead displacement at 0.5 mm, 1.0 mm and 1.5 mm.

		0.5 mm Displacement			1.0 mm Displacement			1.5 mm Displacement		
Collar	**CB(mm)**	**n**	**Mean Force (N)**	**SD**	**n**	**Mean Force (N)**	**SD**	**n**	**Mean Force (N)**	**SD**
No-Collar	1.0	5	111.740	6.0916	5	144.380	4.1919	5	147.060	14.7852
	1.5	5	119.220	7.9641	5	168.880	11.9091	5	187.380	8.0906
	2.0	5	127.640	34.0000	5	184.320	38.4543	4	198.075	44.2871
	Total	15	119.533	20.1049	15	165.860	27.5279	14	176.036	32.5867
Collar	1.0	5	145.700	25.1369	5	199.760	26.1993	5	224.160	21.8344
	1.5	5	129.680	18.9852	5	202.000	38.6238	5	254.520	45.7218
	2.0	5	197.620	33.9269	5	292.660	31.1627	4	347.625	18.6684
	Total	15	157.667	38.9018	15	231.473	53.9102	14	270.279	60.2052

Table 4. Data table for dependent variables Force Resistance at Yield Point, MIT and Slope.

		Force at Yield Point			MIT			Slope		
Collar	CB(mm)	n	Mean Force (N)	SD	n	Mean Torque (Ncm)	SD	n	Mean	SD
No-Collar	1	5	87.28	26.5282	5	18.84	1.992	5	251.26	39.877
	1.5	5	93.22	26.4193	5	26.16	1.992	5	273.956	30.914
	2	5	93.88	49.3597	5	24.18	3.5675	5	264.54	67.277
	Total	15	91.46	33.2572	15	23.06	4.018	15	263.252	45.972
Collar	1	5	105.52	15.8303	5	21.4	1.7903	5	354.98	74.613
	1.5	5	116.16	19.7257	5	25.1	3.0183	5	283.428	64.928
	2	5	187.42	27.8858	5	29.36	5.207	5	389.3	68.377
	Total	15	136.367	42.6787	15	25.29	4.7538	15	342.569	78.835

Table 5. Analysis of variance table for force at crosshead deflection .5 mm.

Source	df	Mean Square	F	p	Observed Power
Collar	1	10906.133	19.247	0.000	0.988
CB Thickness	2	4376.389	7.723	0.003	0.920
Collar * CB Thickness	2	2246.800	3.965	0.033	0.655
Error	24	566.645			
Total	30				

Note: df = degrees of freedom, F = F ratio, p = Type I error probability of given F ratio

Table 6. Analysis of variance table for force at crosshead deflection 1.0 mm.

Source	df	Mean Square	F	p	Observed Power
Collar	1	32288.321	40.466	0.000	1.000
CB Thickness	2	12341.126	15.467	0.000	0.998
Collar * CB Thickness	2	3732.632	4.678	0.019	0.731
Error	24	797.909			
Total	30				

Note: df = degrees of freedom, F = F ratio, p = Type I error probability of given F ratio

Table 7. Analysis of variance table for force at crosshead deflection 1.5 mm.

Source	df	Mean Square	F	p	Observed Power
Collar	1	66394.280	79.667	0.000	1.000
CB Thickness	2	16950.810	20.339	0.000	1.000
Collar * CB Thickness	2	4344.433	5.213	0.014	0.774
Error	22	833.397			
Total	28				

Note: df = degrees of freedom, F = F ratio, p = Type I error probability of given F ratio

Table 8. Analysis of variance table for yield point force.

Source	df	Mean Square	F	p	Observed Power
Collar	1	15124.565	17.267	0.000	0.979
CB Thickness	2	5533.180	6.317	0.006	0.856
Collar * CB Thickness	2	4448.558	5.079	0.014	0.768
Error	24	875.904			
Total	30				

Note: df = degrees of freedom, F = F ratio, p = Type I error probability of given F ratio

Table 9. Analysis of variance table for maximum insertion torque (MIT).

Source	df	Mean Square	F	p	Observed Power
Collar	1	37.185	3.713	0.066	0.456
CB Thickness	2	126.470	12.628	0.000	0.992
Collar * CB Thickness	2	24.544	2.451	0.108	0.445
Error	24	10.015			
Total	30				

Note: df = degrees of freedom, F = F ratio, p = Type I error probability of given F ratio

Table 10. Analysis of variance table for slope of the loading pattern during deformation.

Source	df	Mean Square	F	p	Observed Power
Collar	1	47184.295	13.149	0.001	0.935
CB Thickness	2	5815.179	1.621	0.219	0.308
Collar * CB Thickness	2	9423.621	2.626	0.093	0.472
Error	24	3588.406			
Total	30				

Note: df = degrees of freedom, F = F ratio, p = Type I error probability of given F ratio

Table 11. Data summary table for ESPI calculations.

Cortical Bone Thickness (mm's)	Collar	Load	Specific Strain at 2.0mm (με/N)	Specific Strain Zero Point (mm)	Slope	Displacement (μm/N)
2.0	Yes	M	12.45	2.91	13.68	1.02
2.0	Yes	M	27.08	4.67	10.14	1.37
2.0	Yes	I	3.24	2.85	3.81	0.66
2.0	Yes	I	7.63	2.91	8.38	0.92
2.0	No	M	37.50	3.25	30.00	1.83
2.0	No	M	30.00	4.37	12.66	2.07
2.0	No	I	8.00	2.95	8.42	1.57
2.0	No	I	6.75	3.17	5.77	1.49

Load: (M) mini-implant loaded multiple times (I) mini-implant initially loaded

REFERENCES

Adell R, Lekholm U, Rockler B, Branemark P. A 15-year study of osseointegrated implants in the treatment of the edentulous jaw. Int J Oral Surg 1981;6:387-416.

Akin-Nergiz N, Nergiz I, Schulz A, Arpak N, Niedermeier W. Reactions of peri-implant tissues to continuous loading of osseointegrated implants. Am J Orthod Dentofacial Orthoped 1998; 114:292-298.

Albrektsson T, Lekholm U. Osseointegration: current state of the art. Dent Clin North Am 1989;33:537-54.

Berens A, Wiechmann D, Rudiger J, Skeletal anchorage in orthodontics with mini- and microscrews. Int Orthod 2005;3:325-43.

Bouillaquet s, Gamba J, Forchelet J, Krejci I, Wataha H. Dynamics of composite polymerization mediates the development of cuspal strain. Dent Mater 2006;22:896-902.

Brettin BT, Grosland NM, Qian F, Southard KA, Stuntz TD, Morgan TA, et al. Bicortical vs monocortical orthodontic skeletal anchorage. Am J Orthod Dentofacial Orthop 2008;134:625-35.

Buchter A, Kleinheinz J, Wiesmann H, Kersken J, Weytother H, Neinkemper M, Joos U, Meyer U. Biological and biomechanical evaluation of bone remodeling and implant stability after using an osteome techique. Clin Oral Implants Res 2004 ;12 X.

Buchter A, Weichmann D, Koerdt S, Wiesmann HP, Piffko J, Meyer U. Load related implant reaction of mini-implants used for orthdontic anchorage. Clin Oral Implants Res 2005;16:473-9.

Carter DR, Beaupre GS, Giori NJ, Helmes JA. Mechanobiology of skeletal regeneration. Clin Orthop Relat Res 1998; 335(suppl):S41-S45.

Cheng SJ, Tseng IY, Lee JJ, Kok SH. A prospective study of the risk factors associated with failure of mini-implants used for orthodontic anchorage. Int J Oral Maxillofac Implants 2004:19:100-6.

Chung, 2000; success rates

Costa A, Raffaini M, Melsen B. Miniscrews as orthodontic anchorage; a preliminary report. Int J Adult Orthod Orthognath Surg 1998;13:201-209.

Dabney CL, Dechow PC. Variations in cortical material properties throughout the human dentate mandible. Am J Phys Antropol 2003:120:252-277.

Dalstra M, Catte\aneo PM, Melsen B. Load transfer of miniscrews for orthodontic anchorage.Orthodontics2004;1:53-62.

Deguchi T, Nasu M, Murakami K, Yabuuchi T, Kamioka H, Yamamoto T. Quantitative evaluation of cortical bone thickness with computed tomographic scanning for orthodontic implants. Am J Orthod Dentofac Orthoped 2006;129:721.e7-721.e12.

Fritz U, Diedrich P, Kinzinger G, Al-Said M. The anchorage quality of mini-implants towards translatory and extrusive forces. J Orofac Orthop 2003;64:293-304.

Fritz U, Ehmer A, DIedrich P. Clinical suitability if titanium microscrews for orthodontic anchorage – preliminary experiences. J Orofac Orthop 2004;65:410-8.

Freudenthaler JW, Haas R, Bantleon HP. Bicortical titanium screws for critical orthodontic anchorage in the mandible: a preliminary report on clinical applications. Clin Oral Implants Res 2001;12:358-63.

Frost HM. Skeletal structural adaptations to mechanical usage (SATMU): 1. Redefining Wolff's law: the bone modeling problem. Anat Rec 1990a;226:403-413.

Frost HM. Wolff's law and bone's structural adaptationds to mechanical useage: an overview for clinician's. Angle Orthod 1994;64:175-88.

Garfinkle JS, Cunningham LL, Beeman CS, Kluemper GT, Hicks EP, Kim MO. Evaluation of orthodontic mini-implant anchorage in premolar extraction therapy in adolescents. Am J Orthod Dentofacial Orthop 2008;33:642-653.

Goaslind GD, Robertson PB, Mahan CJ, Morrison WW, Olson JV. Thickness of facial gingiva. J Periodontol 1977;48:768-71.

Huja SS, Litsky AS, Beck FM, Johnson KA, Larsen PE. Pull-out strength of mono-cortical screws placed in the maxillae and mandible of dogs. Am J Orthod Dentofacial Orthop 2005;127:307-13.

Hurzler MB, Qumones CR, Kohal RJ, Rohde M, Slurb JR, Teusher U. Changes in peri-implant tissue subjected to orthodontic forces and ligature breakdown in monkeys. J Periodont 1998;69:396-404.

Isidor F. Histological evaluation of peri-implant bone at implants subjected to occlusal overload or plaque accumulation. Clin Oral Implants Res 1997;8:1-9.

Janssen, Raghoebar, Vissink, Sandham. Skeletal anchorage in orthodontics – a review of various systems in animal and human studies. Int J Oral Maxillofacial Implants 2008;23:75-78.

Jones, R., Wykes, C., 1989. Electronic Speckle Pattern Correlation Interferometry. Cambridge University Press, Cambridge.

Kanomi R. Mini-implant for orthodontic anchorage. J Clin Orthod 1997;31:763-7.

Kim 2002, mini success

Kim JW, Baek S, Kim TW, Chang Y. Comparison of stability between cylindrical and conical type mini-implants. Angle Orthod 2008;78:692-8.

Kircelli BH, Pekta ZO, Uckan S. Orthopedic protraction with skeletal anchorage in a patient with maxillary hypoplasia and hypodontia. Angle Orthod 2005;76:156-63.

Kishen A, Murukeshan VM, Krishnakumar V, Asundi A. Analysis of the nature of thermally induced deformation in human dentine by electronic speckle pattern interferometry (ESPI). J Dent 2001;29:531-7.

Kuroda S, Katayama A, Takano-Yamamoto T. Severe anterior open-bite case treated using titanium screw anchorage. Angle Orthod 2004;74:558-67.

Kuroda S, Sugawara Y, Deguchi T, Kyung HM, Yamamoto TT. Clinical use of miniscrew implants as orthodontic anchorage: Success rates and postoperative discomfort. AM J Orthod Dentofacial Orthop 2007;131:9-15.

Liou EJ, Pai BC, Lin JC. Do miniscrews remain stationary under orthdontic forces? Am J Orthod Dentofacial Orthop 2004;126:42-7.

Majzoub Z, Finotti M, Miotti F, Giardino R, Aldini NN, Cordioli G. Bone response to orthodontic loading of endosseous implants in the rabbit calvaria: early and continuous distalizing forces. Eur J Orthod 1999;21:223-30.

Melsen B. A rational approach to orthodontic anchorage. Prog Orthod 1999;1:10-22

Melsen B, Costa A. Immediate loading of implants used for orthodontic anchorage. Clin Orthod Res 2000;3:23-8.

Melsen B, Verna C. Miniscrew implantsa: the Aarhus anchorage system. Sem in Orthod 2005;11(1):24-31.

Melsen B. Mini-implants: where are we? J Clin Orthod 2005;39:539-47.

Mihalko WM, May TC, Kay JF, Krause WR. Finite element analysis of interface geometry effects on the crestal bone surrounding a dental implant. Implant Dentistry Fall 1992;1:212-217.

Misch CE. Bone character: a second vital implant criterion. Dent Today 1988;7:39-40.

Misch CE. Contemporary Implant Dentistry. 2nd ed. St. Louis:Mosby; 1998.

Misch CE, Qu Z, Bidez M. Mechanical properties of trabecular bone in the human mandible: Implications for dental implant treatment planning and surgical placement. J Oral Maxillofac Surg 1999;57:700-706.

Miyawaki S, Koyama I, Inoue M, Mishima K, Sugahara T, Yakano-Yamamoto T. Factors associated with the stability of titanium screws placed in the posterior region for orthodontic anchorage. Am J Orthod Dentofacial Orthop 2003;124:373-8.

Moon CH, Lee DG, Lee HS, Im JS, Baek SH. Factors associated with the success rate if orthodontic miniscrews placed in the upper and lower posterior buccal regions. Angle Orthod 2008;78:101-106.

Morarend C, Qian F, MarshaLL SD, Southard KA, Grosland NM, Morgan TA McManus M, Southard TE. Effect of screw diameter on orthodontic skeletal anchorage. Am J Orthod Dentofacial Orthop 2009;136:224-229.

Motoyoshi M, Yano S, Tsuruoka T, Shimizu N. Biomechanical effect of abutment on stability of orthodontic mini-implant. A finite element analysis. Clin Oral implants Res 2005,16:480-485.

Motoyoshi M, Yoshida T, Ono A, Shimizu N. Effect of cortical bone thickness and implant placement torque on stability of orthodontic mini-implants. Int J Oral Maxillofac Implants 2007; 22:779-784.

Muller HP, Eger T. Masticatory mucosa and periodontal phenotype: a review. Int J Periodontics Restorative Dent 2002;2:172-83.

Murukeshan VM, Ganesan AR, Sirohi RS, Malhotra SK. Non-destructive evaluation of fiber reinforced polymer composite by an all fiber optic phase shifting electronic speckle pattern interferometer. SPIE 1996;2921:101-7.

Ohmae M, Saito S, Morohashi T, Seki K, Qu H, Kanomi R, et al. A clinical and histological evaluation of titanium mini-implants as anchors for orthodontic intrusion in the beagle dog. Am J Orthod Dentofacial Orthop 2001;119:489-97.

Ono A, Motoyoshi M, Shimizu N. Cortical bone thickness in the buccal posterior region for orthodontic mini-implants. Int J Oral Maxillofac Surg 2008;37:334-340.

Park HS, Bae SM, Kyung HM, Sung JH. Micro-implant anchorage for treatment of skeletal Class I bialveolar protrusion. J Clin Orthod 2001;35:417-22.

Park HS, Kyung HM, Sung JH. A simple method of molar uprighting with micro-implant anchorage. J Clin Orthod 2002;36:592-6.

Park HS, Jeong SH, Kwon OW. Factors affecting the clinical success of screw implants used as orthodontic anchorage. Am J Orthod Dentofacial Orthop 2006;130:18-25

Park HS, Lee YJ, Jeong SH, Kwon TG. Density of alveolar and basal bones of the maxilla and mandible. Am J Orthod Dentofacial Orthop 2008;133:30-37.

Reid, G.T. Automatic fringe pattern analysis: a review. Opt. Laser. Eng 1986;7:37-68.

Ren Y. Optimum force magnitude for orthodontic tooth movement: a systematic review. Angle Orthod. 2003; 73:86-92.

Roberts WE, Helm FR, Marchalkl KJ, Gongloff RK. Rigid endosseous implants for orthodontic and orthopedic anchorage. Angle Orthod 1989;59:247-256.

Roberts WE, Nelson CL, Goodacre CJ. Rigid implant anchorage to close a mandibular first molar extraction site. J Clin Orthod 1994;27:693-704.

Romanos GE, Toh CG, Siar CH, Swaminathan D. Histologic and histomorphometric evaluation of peri-implant bone subjected to immediate loading: an experiemtal study with Macaca fascicularis. Int J Oral Maxillofac Implants 2002;17:44-51.

Sevinmay M, Turhan F, Kilicarlslan MA, Eskitascioglu G. Three-dimensional finite element analysis of the effect of different bone quality on stress distribution in an implant-supported crown. J Prosthet Dent 2005;93:227-234.

Seong WJ, Kim UK, Swift J, Heo YC, Hodges JS, Ko CC. Elastic properties and apparent density of human edentulous maxilla and mandible. In J Oral Maxillofac Surg 2009 (in press)

Shahar R, Insights into whole bone and tooth function using optical metrology, J Mater Sci 2007; 42:8919-8933.

Simmons CA, Meguid SA, Pillar RM. Mechanical regulation of localized and appositional bone formation around bone-interfacing implants. J Biomed Mater Res 2001;55:63-71.

Wehrbein H, Diedrich P. Endosseous titanium implants during and after orthodontic load – an experimental study in the dog. Clin Oral Imp Res 1993;4:76-82.

Wehrbein H, Glatzmaier J, Yilditim M. Orthodontic anchorage capacity of short titanium screw implants in the maxilla. An experimental study in the dog. Clin Oral Implants Research 1997;8: 131-141.

Szmukler-Moncler S, Salama H, Reingewirtz Y, Dubruille JH. Timing of the loading and effect of micromotion on bone-dental implant interface: review of experimental literature. J Biomed Mater Research 1998;43:193-203.

Stahl E, Numerical anal of biomech, J Orofac Orthoped 2009;70:115-27 in book

Weichman 2007

Wilmes B, Impact of implant design on primary stability of orthodontic mini-implants. 2008. J Orofac Orthop. 69:42-45. In book

Woo, 2003 success rates

Yap AU, Tan AC, Quan C. Non-destructive characterization of resin-based filling materials using Electronic Speckle Pattern Interferometry. Dent Mater 2004;20:377-82.

Zalansky P, Friesman A, Weiner S. Structure and mechanical properties of the soft zone separating bulk dentin and enamel in crowns of human teeth. J Struct Biol 2006;153:188-199.

(Serra, 2008).

(Pilliar RM *et al., 2005).*

(Cheal *et al.,* 1991; Meyer *et al.,* 1999). Cell formation and bone remodeling

Melsen and Verna, 2005 mini-implant failure low bone density

Park YC *et al.,* 2003). Force on implasnts

Melsen, 2005 FEM

Appendix 1.

Table X. Data summary table for mechanical testing.

Sample	Collar	Cortical Bone (mm)	MIT (N/cm)	Yield Point (N)	Peak Load (N)	Modulus	Force to Displacement (N)		
							0.5mm	1.0mm	1.5mm
1	Yes	1	20.7	112.5	254.9	414.8	173.9	231	251.8
2	Yes	1	23.3	102.7	246	259.9	130.8	206.4	239.7
3	Yes	1	21.4	83.6	201.9	327.5	122.3	178.4	199.7
4	Yes	1	18.8	126.8	225.5	445.2	172.1	215.3	222.8
5	Yes	1	22.8	102	209.5	327.5	129.4	167.7	206.8
6	No	1	20.5	53.8	143.2	310.9	114.3	143.7	122.3
7	No	1	17.7	100.1	153	213.8	104.1	143.2	152.6
8	No	1	19.7	64.5	149.9	239.3	109.9	145	149.9
9	No	1	15.9	114.8	162.4	270.7	120.5	150.8	161.9
10	No	1	20.4	103.2	151.2	221.6	109.9	139.2	148.6
11	Yes	1.5	23.8	129.3	295.1	286.94	129.3	210.1	273
12	Yes	1.5	23.4	127.4	261	222.41	112.4	175.3	231.4
13	Yes	1.5	30.2	83.6	316.5	386.77	151.1	233.5	293.5
14	Yes	1.5	22.7	111.2	239.8	234.08	109.4	150.2	185.5
15	Yes	1.5	25.4	129.3	306.7	286.94	146.2	240.9	289.2
16	No	1.5	25.7	98.4	203.8	296.55	128.5	180	199.2
17	No	1.5	23.8	66	183.9	296.55	114.8	163.3	181
18	No	1.5	27.9	113.6	190.6	295.77	126.3	182.2	190.9
19	No	1.5	28.5	122.4	189.6	246.83	116.9	164.8	186.7
20	No	1.5	24.9	65.7	164.4	234.08	109.6	154.1	179.1
21	Yes	2	31.2	224.2	372.3	404	224.2	318.9	365.2
22	Yes	2	35.3	199.6	347.3	370.7	183	299.3	345.2
23	Yes	2	28.3	148.1	349.6	306.9	153.5	240.6	322.5
24	Yes	2	30.8	179.7	373.2	370.7	189	290.9	357.6
25	Yes	2	21.2	185.5	323.4	494.2	238.4	313.6	N/A
26	No	2	22.1	31.2	204.2	247.1	115.2	190.8	N/A
27	No	2	23.9	83.6	168.6	261.8	120.5	157	167.7
28	No	2	19.6	72.1	157.9	164.7	81.4	134.3	152.6
29	No	2	26.8	121.9	233.1	342.2	168.1	227.3	233.1
30	No	2	28.5	160.6	245.1	306.9	153	212.2	238.9

N/A Data point not recorded